

PL-TR-91-2161

AD-A240 814



①

DEVELOPMENT OF A COMPREHENSIVE SEISMIC YIELD ESTIMATION SYSTEM FOR UNDERGROUND NUCLEAR EXPLOSIONS

J.R. Murphy
J.L. Stevens
D.C. O'Neill
B.W. Barker
K.L. McLaughlin
M.E. Marshall

S-CUBED

A Division of Maxwell Laboratories, Inc.

P.O. Box 1620

La Jolla, CA 92038-1620

May, 1991

Scientific Report No.2

DTIC
ELECTE
SEP 26 1991
S B D

APPROVED FOR PUBLIC RELEASE; DISTRIBUTION UNLIMITED.

91-11665




PHILLIPS LABORATORY
AIR FORCE SYSTEMS COMMAND
HANSCOM AIR FORCE BASE, MA 01731-5000

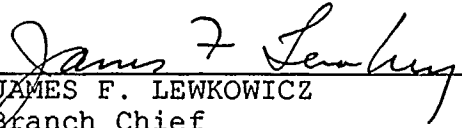
SPONSORED BY
Defense Advanced Research Projects Agency
Nuclear Monitoring Research Office
ARPA ORDER NO. 5307


MONITORED BY
Phillips Laboratory
Contract FY19628-89-C-0026

The views and conclusions contained in this document are those of the authors and should not be interpreted as representing the official policies, either expressed or implied, of the Defense Advanced Research Projects Agency or the U.S. Government.

This technical report has been reviewed and is approved for publication.


JAMES F. LEWKOWICZ
Contract Manager
Solid Earth Geophysics Branch
Earth Sciences Division


JAMES F. LEWKOWICZ
Branch Chief
Solid Earth Geophysics Branch
Earth Sciences Division


DONALD H. ECKHARDT, Director
Earth Sciences Division

This report has been reviewed by the ESD Public Affairs Office (PA) and is releasable to the National Technical Information Service (NTIS).

Qualified requestors may obtain additional copies from the Defense Technical Information Center. All others should apply to the National Technical Information Service.

If your address has changed, or if you wish to be removed from the mailing list, or if the addressee is no longer employed by your organization, please notify PL/IMA, Hanscom AFB, MA 01731-5000. This will assist us in maintaining a current mailing list.

Do not return copies of this report unless contractual obligations or notices on a specific document requires that it be returned.

Original contains color
plates: All DTIC reproductions
will be in black and
white

REPORT DOCUMENTATION PAGE

| | | | | | |
|--|-------|--|--|------------------------|---------------------------|
| 1a. REPORT SECURITY CLASSIFICATION UNCLASSIFIED | | | 1b. RESTRICTIVE MARKINGS None | | |
| 2a. SECURITY CLASSIFICATION AUTHORITY UNCLASSIFIED | | | 3. DISTRIBUTION / AVAILABILITY OF REPORT Approved for Public Release; Distribution Unlimited | | |
| 2b. DECLASSIFICATION / DOWNGRADING SCHEDULE UNCLASSIFIED | | | | | |
| 4. PERFORMING ORGANIZATION REPORT NUMBER(S) SSS-TR-91-12434 | | | 5. MONITORING ORGANIZATION REPORT NUMBER(S) PL-TR-91-2161 | | |
| 6a. NAME OF PERFORMING ORGANIZATION S-CUBED, Division of Maxwell Laboratories, Inc. | | 6b. OFFICE SYMBOL (if applicable) | 7a. NAME OF MONITORING ORGANIZATION Phillips Laboratory | | |
| 6c. ADDRESS (City, State, and ZIP Code) P.O. Box 1620 La Jolla, California 92038-1620 | | | 7b. ADDRESS (City, State, and ZIP Code) Hanscom Air Force Base Massachusetts 01731-5000 | | |
| 8a. NAME OF FUNDING / SPONSORING ORGANIZATION DARPA | | 8b. OFFICE SYMBOL (if applicable) NMRO | 9. PROCUREMENT INSTRUMENT IDENTIFICATION NUMBER FI9628-89-C-0026 | | |
| 8c. ADDRESS (City, State, and ZIP Code) 1400 Wilson Boulevard Arlington, Virginia 22209-2308 | | | 10. SOURCE OF FUNDING NUMBERS | | |
| | | | PROGRAM ELEMENT NO. 62714E | PROJECT NO. 9A10 | TASK NO. DA |
| 11. TITLE (Include Security Classification) DEVELOPMENT OF A COMPREHENSIVE SEISMIC YIELD ESTIMATION SYSTEM FOR UNDERGROUND NUCLEAR EXPLOSIONS | | | | | |
| 12. PERSONAL AUTHOR(S) J.R. Murphy, J.L. Stevens, D.C. O'Neill, B.W. Barker, K.L. McLaughlin, M.E. Marshall | | | | | |
| 13a. TYPE OF REPORT Scientific Report No.2 | | 13b. TIME COVERED FROM 900200 TO 910200 | 14. DATE OF REPORT (Year, Month, Day) 1991 May | | 15. PAGE COUNT 36 |
| 16. SUPPLEMENTARY NOTATION | | | | | |
| 17. COSATI CODES | | | 18. SUBJECT TERMS (Continue on reverse if necessary and identify by block number) | | |
| FIELD | GROUP | SUB-GROUP | | | |
| | | | Nuclear Explosions Software System X Window | | |
| | | | Yield Estimation Shagan River YES | | |
| | | | Seismic JVE CSS | | |
| 19. ABSTRACT (Continue on reverse if necessary and identify by block number) | | | | | |
| <p>This report summarizes the progress which has been achieved during the past year in the development of a comprehensive new seismic yield estimation system for underground nuclear explosions. Specifically, a preliminary prototype version of this system, which has now been successfully implemented at the DARPA Center for Seismic Studies (CSS), is described in detail and its functionality is graphically illustrated through a sample application to the seismic data recorded from a selected explosion.</p> <p>The software system design criteria are reviewed in Section 2, where the characteristics of the data, analysis tools, database management system and graphical user interface are described in the context of their integration into a comprehensive system for seismic yield estimation and compliance assessment. This discussion includes an overview of the conceptual model for the system and provides a description of how the prototype version has been implemented in a SUN color workstation environment using software built upon the framework of the X Window graphics and Oracle database management systems.</p> <p style="text-align: right;">(continued on reverse)</p> | | | | | |
| 20. DISTRIBUTION / AVAILABILITY OF ABSTRACT <input checked="" type="checkbox"/> UNCLASSIFIED/UNLIMITED <input type="checkbox"/> SAME AS RPT. <input type="checkbox"/> DTIC USERS | | | 21. ABSTRACT SECURITY CLASSIFICATION UNCLASSIFIED | | |
| 22a. NAME OF RESPONSIBLE INDIVIDUAL James F. Lewkowicz | | | 22b. TELEPHONE (Include Area Code) 617/377-3222 | | 22c. OFFICE SYMBOL LWH |

19. ABSTRACT (Continued)

This is followed in Section 3 by a demonstration of system capabilities in which a complete processing session is graphically illustrated using data recorded from the Joint Verification Experiment (JVE) which was conducted at the Soviet Shagan River test site on 14 September 1988. In this presentation, reproductions of the actual workstation screens encountered by an analyst in such a session are used as a framework for describing the simple menu driven structure on which the graphical user interface has been developed. Among other features, this demonstration is used to illustrate the manner in which available test site information is presented to the analyst in the context of a SPOT[®] satellite image of the test site, in a format which permits the analyst to interact digitally with the image in a workstation environment to create overlays to and cross-sections through the image to display event locations, topography, surface and subsurface geologic data and a variety of geophysical parameters of potential interest in yield estimation analysis. In addition, this sample session is used to illustrate the capabilities provided by the system which permit the analyst to interact with the recorded seismic data to process it and extract the various magnitude measures of interest, to formally combine these seismic measures of source size to obtain an optimum measure of explosion yield and quantitative measures of the associated uncertainty and to statistically assess the consistency of the unified seismic yield estimate with any existing treaty thresholds or other yield levels of particular interest.

Table of Contents

| SECTION | PAGE |
|---|------|
| 1 Introduction | 1 |
| 2 YES Software Design | 3 |
| 2.1 Conceptual Model | 3 |
| 2.2 Implementation Framework | 4 |
| 2.3 Database Structure | 5 |
| 2.4 Database Contents | 6 |
| 3 Overview of System Capabilities | 8 |
| 4 Summary and Future Plans | 33 |
| 4.1 Summary | 33 |
| 4.2 Future Plans | 33 |
| Acknowledgements | 35 |
| References | 36 |



Original contains color
plates: All DTIC reproductions
will be in black and
white.

| | |
|---------------------|-------------------------------------|
| Accession For | |
| NTIS GRA&I | <input checked="" type="checkbox"/> |
| DTIC TAB | <input type="checkbox"/> |
| Unannounced | <input type="checkbox"/> |
| Justification | |
| By _____ | |
| Distribution/ _____ | |
| Availability Codes | |
| Dist | Avail and/or Special |
| A-1 | |

List of Illustrations

| FIGURE | | PAGE |
|--------|--|------|
| 1 | Main menu structure for YES..... | 8 |
| 2 | Illustration of pulldown access to individual menu functions. | 9 |
| 3 | SPOT satellite image of the Shagan River test site with superimposed locations of the historical explosions (squares) and current event (diamond). | 10 |
| 4 | Full resolution SPOT satellite image of the region surrounding the Shagan River cratering explosion of 15 January 1965. | 11 |
| 5 | Illustration of interactive modification of brightness and contrast in SPOT satellite image display. | 11 |
| 6 | SPOT satellite image of the Shagan River test site with superimposed surface geologic map and current event location. | 12 |
| 7 | Color-coded representation of DMA topographic data for the Shagan River test site with superimposed topographic contours and current event location. | 13 |
| 8 | Vertical subsurface section through the current event shotpoint along the interactively selected line shown on the SPOT image insert. | 13 |
| 9 | Color-coded representation of depth to the top of the granite surface beneath the Shagan River test site with superimposed depth contours and current event location. | 14 |
| 10 | World map projections ($\Delta < 100^\circ$) showing locations of stations for which digital teleseismic P (left) and L_g (right) data are available for the current event. | 15 |
| 11 | Analyst station display of vertical-component L_g signals for the current event. | 16 |
| 12 | Magnitude measurement menu. | 16 |
| 13 | Analyst station display of selected vertical-component teleseismic P wave signals for the current event. | 17 |
| 14 | Example of the specification and subsequent application of a bandpass filter to the data of Figure 13. | 18 |

| | | |
|----|---|----|
| 15 | SPOT locations of Shagan River explosions recorded at station KONO in Norway. The diamond symbols denote those events selected for comparative analysis. | 19 |
| 16 | Comparison of the P wave signal recorded at station KONO from the current event (top and red) with the signals recorded at that station from the selected events of Figure 15. | 20 |
| 17 | Illustration of the interactive determination of the amplitude and period values used to define single station m_b values. | 21 |
| 18 | Comparison of individual station and network-averaged m_b magnitudes determined for the current event. | 21 |
| 19 | Comparison of individual station and network-averaged M_{Lg} magnitudes determined for the current event. | 22 |
| 20 | Comparison of the observed value of $m_b - M_{Lg}$ (NORSAR) for the current event with contours representing observed variation of that parameter for previous events. | 22 |
| 21 | Analyst station display of selected long-period Rayleigh wave signals for the current event. | 23 |
| 22 | Example of the specification and subsequent application of the instrument response normalization feature to the data of Figure 21. | 24 |
| 23 | Menu options for the estimation of network-averaged P wave spectra. | 25 |
| 24 | Comparison of normalized observed and best-fitting theoretical network-averaged P wave spectra for the current event. | 25 |
| 25 | Comparison of the inferred surface wave moment tensor solution for the current event with the corresponding path-normalized, observed Rayleigh (left) and Love (right) wave amplitude data. | 26 |
| 26 | Comparison of the surface wave moment tensor solution for the current event (yellow and light blue concentric circles) with those for nearby Shagan River explosions (red and dark blue concentric circles) and with the surface geologic map of the area. | 27 |
| 27 | Meru and sample output for the unified yield estimation module. | 28 |

FIGURE

PAGE

| | | |
|----|--|----|
| 28 | Comparison of unified yield estimates (W) and associated uncertainties (F) obtained with (top) and without (bottom) the surface wave moment tensor magnitude. | 29 |
| 29 | Statistical assessment menu. | 29 |
| 30 | Comparison of the results of three different tests of seismic compliance of the current event with the 150 kt threshold of the TTBT. | 30 |
| 31 | Compliance test result (Test 1) for the scenario in which the current event data were observed from an explosion below the water table at NTS. | 30 |
| 32 | Spreadsheet summary comparison of seismic yield estimates for the current event (09/14/88) with those obtained for selected previous Shagan River explosions. | 31 |
| 33 | Spreadsheet summary illustrating the results of interactively modifying the designed magnitude/yield relations. | 32 |

1 Introduction

Research conducted over the past decade has led to the development of a number of innovative procedures for estimating the yields of underground nuclear explosions through systematic analyses of digital seismic data recorded from these tests. In addition, a wide variety of new data regarding the geophysical environments at Soviet test locations have now become available as a result of the Joint Verification Experiment (JVE) and associated data exchanges. The objective of the research program described in this report is to integrate all these new capabilities and data into a comprehensive, prototype system which can be used to derive optimum seismic estimates of explosion yield. More specifically, it is to implement a flexible interactive software system in which yield estimates based on a wide variety of different seismic magnitude measurements can be efficiently determined, merged with all available information regarding the test location under consideration and statistically combined to obtain a unified seismic estimate of explosion yield and quantitative measures of the uncertainty in that estimate.

A preliminary prototype version of a system designed to achieve the above objectives, designated the Yield Estimation System (YES), has been implemented in a Sun color workstation (SPARCStation) environment at the DARPA Center for Seismic Studies (CSS) using software built upon the framework of the X Window graphics and Oracle database management systems. This initial version focuses on explosions at the Soviet

Shagan River test site and on yield estimates based on five different seismic magnitude measures derived from teleseismic P and surface wave (m_b , M_{Pspec} , M_0) and regional L_g and P wave (M_{Lg} , M_{Pn}) data. Available test site information is presented to the analyst in the context of a SPOTTM satellite image of the Shagan River region, in a format which permits the analyst to interact digitally with the image to easily extract and display information regarding the explosion source environment. A waveform database consisting of more than 10000 digital seismograms recorded from Shagan River explosions at stations of the GDSN, USAEDS, NORSAR, CDSN and IRIS networks has been assembled for this system. The graphical user interface to this system is completely menu-driven and mouse-activated and has been designed so that no keyboard entry is required of the operator. Thus, the seismic data can be directly input to the various data processing modules using a simple menu selection procedure to obtain the magnitude measures and associated yield estimates.

This report presents a summary of the current status of the ongoing research investigations directed toward the development of an improved seismic yield estimation capability for underground explosions. The system design criteria are reviewed in Section 2, where the characteristics of the data, analysis tools, database relations and graphical user interface are described in the context of their integration into a comprehensive software system. This is followed in Section 3 by

TM SPOT data are copyrighted by CNES (1986,1987).

an overview of system capabilities in which the functionality of the current prototype system is graphically illustrated using displays of the screens encountered by an analyst in a typical processing

session for a selected (i.e., the JVE) explosion. The report concludes with Section 4 which contains a summary and a discussion of future plans for the development of the YES.

2 YES Software Design

The YES is designed to determine an optimum explosion yield, the uncertainty in this yield, and a statistical assessment of the results, using a wide variety of analysis tools applied to seismic signals generated by underground nuclear explosions. Such a system requires a flexible design that allows analysis tools to be easily added and yet allows all or part of the analysis tools and all or part of the data to be used for any given yield estimate. Furthermore, because the yield estimates depend on several types of analysis and a variety of data which will not only vary from one event to the next, but will also change as new data becomes available for a single event, the system must allow identification of all of the data and processing steps that correspond to any yield estimate made with the system.

In this section of this report, we discuss the YES software design, the conceptual model for the system, the requirements and constraints of the system, how the database has been designed to handle general analysis tools and how the system has been structured to achieve design goals. This is intended to provide a description of the underlying structure of the system that forms a platform for operation of YES modules.

2.1 Conceptual Model

YES is an example of a general class of systems built on four basic elements.

- data
- analysis tools
- a database management system
- a graphical user interface.

In this case the data include seismic waveform data from underground nuclear explosions, related data such as event locations and material properties at test sites, parametric data such as magnitudes derived from seismic data, historical data, and image data. The analysis tools operate on these data and extract and/or display information. Examples of analysis tools are programs to display waveforms, measure magnitudes, and overlay event and geographic information on maps and images. The data and all of the analysis results up to and including the inferred explosion yield are maintained within a relational database management system. This system performs both the function of keeping track of raw data and related information and the function of maintaining a processing history of each yield estimate. The graphical user interface allows the user to interact with the data, database, and analysis tools. All user interaction takes place through the graphical user interface. For YES, this interface has been designed to minimize the amount of keyboard entry and to allow nearly all selection to occur through mouse driven menus and displays.

YES consists of a hierarchy of programs. At the top level is a master program whose primary function is to start the other analysis programs. The top level program allows the user to select the

test site, event, and phase to be processed, and the analysis tool to apply to the data corresponding to that selection. It then starts the analysis program with the proper input. The master program starts some processes automatically; experience has shown that user time can be saved by running certain computationally-intensive modules as soon as input data are ready for them. By design, the master program is both small and simple. Because of this, it is easy to expand the program to add additional analysis modules as required.

A difficult problem in the design of the interactive system was to make it robust and easy to use for an operator with limited training while retaining versatility sufficient for an expert to apply the system to complex cases. Our solution to this problem has been to provide user control over operational characteristics of the analysis modules to allow performance of complex operations but also to build in default settings that are appropriate under most circumstances. Thus, a user can operate the system in a routine way by simply following a well-defined set of steps from addition of new data through estimation of explosion yield. However, if special problems occur, such as an anomalous result or the need to modify a yield estimate in response to other knowledge, an expert can adjust the operation of the modules. In either case, the chosen parameters are stored in the database and can be recovered together with the resulting yield estimate at any time.

2.2 Implementation Framework

The graphical user interface of the Yield Estimation System is based on the X Window

System. X was designed specifically to allow hardware independence, to foster ease in porting applications to machines other than those for which they were developed, and to permit running of applications on one computer while displaying their output on another, even if the computers are of different manufacture. YES was designed and implemented on Sun SPARC computers (e.g., SPARCstations), but transfer to any other system that supports X and UNIX could be accomplished easily. The X interface has been written using the X toolkit. The X toolkit enforces an object-oriented approach to programming by combining the windows and the operations on the windows into "widgets". YES uses several widget sets including the Motif widget set from the Open Software Foundation, the X widget set from Hewlett Packard, the Athena widget set from MIT, graphics widgets written by Teledyne-Geotech and SAIC, and special purpose widgets for YES written by S-CUBED.

YES is written in the C and FORTRAN programming languages. C was chosen because programmers' calls to the X Window System procedures are in C, and because C is well suited to the design of complex systems with a variety of data structures. FORTRAN was used because it is optimal for certain types of computational analysis, and because its use permitted the inclusion of many previously existing analysis tools into YES. As a result, the top level programs, interactive modules, database interface, and graphics routines are written in C, and when appropriate these routines call FORTRAN subroutines.

YES uses the Oracle relational database management system as its database manager. Oracle was chosen because it is used as the database manager at the Center for Seismic Studies,

and because it is available for a wide variety of hardware platforms. YES uses a library of procedures to access the database, and all Oracle-specific calls have been isolated so that they can be replaced with a minimum of effort if necessary. The relational database tables are independent of the particular database management system used to store and access the tables. YES can be configured to use an internal database manager if Oracle is not available.

All database tables are documented in a standard format before being created in Oracle or used within the system. All Oracle creation and load scripts as well as the header files that define internal data structures and external file formats are generated directly from the documentation. This way typographic errors are avoided and any changes in the database structure can be made throughout the system by changing only the documentation and regenerating dependent files.

2.3 Database Structure

The Yield Estimation System is constructed on a substrate of a database management system and a database, which serve to manage all data required for communication between modules. Each module extracts what it needs from the database and returns what it concludes to the database. Modules may then interact with the results of other modules by examining data stored in appropriate places.

Seismic data are stored in a manner like that used at the Center for Seismic Studies, i.e. as waveform files and a set of associated tables which

describe each waveform, but with enhancements. The tables used in YES are a superset of those defined in the CSS version 3.0 database specification (Anderson, *et al.*, 1990). Among the additions made at S-CUBED are tables which allow the simultaneous presence of several sets of observed and derived information, along with a facility to specify which of the several sets contains the currently preferred information. This feature's primary purpose is to impart traceback capability, so that an investigator can determine why yield determinations of an event made at several sessions differ. For example, as more stations report their locations for an event, the origin information associated with a set of waveforms may change; previous determinations of yield may have depended upon the origin as it was known at the time, and recreation of those previous results depends upon recovery of the information about origin known at the time. Station and event magnitudes, station corrections, and input to analysis programs are all saved in a way that permits later traceback. Waveforms viewed with the analyst's station always use the currently preferred set of waveform tables.

The database is designed to facilitate data flow between YES analysis modules. In general, the procedure used by analysis programs is to extract waveform and/or tabular data from the database, measure the size of the event, and append the result and all important processing parameters to the database. The analyst station can save arrival times and magnitudes measured on individual waveforms to the database. Some of the magnitude measurement modules retrieve magnitudes derived from individual waveforms and merge them to obtain a network magnitude, while others

examine waveforms directly, without user intervention, then average the results to obtain a single magnitude measure. The yield estimation procedure recovers the results of the magnitude measurement modules from the database and produces a weighted yield for the event. This estimated yield is then compared with yields from other events in the database to derive statistics describing the likelihood that the event under examination was in compliance with or in contravention to existing treaties. All these procedures share their results via the database.

2.4 Database Contents

As mentioned above, the foundation of YES is a comprehensive database that allows a user to extract parameters from explosion waveforms, combine these parameters to obtain an estimate of the explosion yield, and review these results in the context of the environment in which the explosion took place. Such a database necessarily contains a large variety of both seismic and non-seismic data.

The seismic component can be broken down into four major classes of information, these being:

- event and origin (epicentral) information
- waveform and waveform related information
- measurements obtained from the waveforms
- static, tabular information, such as travel-time tables, earth models, station locations and instrumentation.

Each of these major classes by itself can be

further subdivided with finer distinctions. For example, event and origin information is obtained from many classified and unclassified sources, each of which provides the information at different levels of detail. Unclassified locations, origin times and body-wave magnitudes have been obtained from the ISC and NEIS for all explosions. Other origin times and locations, computed using a joint epicenter inversion technique, have been extracted from Marshall *et al.* (1984). Classified seismic locations and magnitudes computed using USAEDS network stations also have been incorporated into the database, as have locations determined by analysis of classified and unclassified satellite photographs. Event yields based on AFTAC analysis of USAEDS waveforms are available for all events, and additional yields are available from the published Soviet literature (Bocharov *et al.*, 1989), from data exchanges with the Soviet government, and in the case of the JVE, by direct measurement.

Sources of waveform data are just as diverse. Waveform data are received routinely from AFTAC, CSS, IRIS, and other sources, and can be further categorized by type, such as short-period, long-period, broadband, single station, array, and 3-component, or by network, such as USAEDS, NORSAR, GDSN, CDSN, and IRIS. As of this date the waveform database contains more than 10000 discrete waveforms and occupies storage of over 300 megabytes (MB). An extensive effort has been made to insure high quality in the waveform database. Thus, every waveform has been visually inspected by a trained analyst to determine waveform quality. In the course of reviewing the data many of the collected waveforms were found to be unusable due to windowing problems, contamina-

tion by other events, timing and calibration errors, spikes, data dropouts and other instrument problems. Thus, it was found that the data preview effort was critically important in the development of a database which would fulfill the goals of this project.

Measurements consist of those produced by the analysis modules within YES itself, as well as measurements received from outside sources, such as AFTAC single-station magnitude measurements. This variety is necessary for performing detailed comparisons between yields derived from YES and those computed by other methods using different data sets.

Tabular information consists of a complete station location file containing both classified and unclassified station locations, standard travel-time tables for the important seismic phases (Herrin *et al*, 1968), surface wave path corrections for use in moment tensor inversion, and a comprehensive instrument response database. The instrument database is a compilation of information collected from the USGS, AFTAC, IRIS, and others which details the characteristics of the recording instruments as a function of station, channel and date. There are currently 750 different response histo-

ries in this section of the database.

In addition to seismic data, the database contains much visual and geologic data. There are approximately 44 MB of SPOT panchromatic image data for the Shagan River test site, some of which has 30m resolution and is used to view the entire test site at once, and most of which has 10m resolution for use in detailed examination of the neighborhood of a particular event. Geologic images, digital topography, and data used in creating cross-sections encompass 12 MB. About 1 MB of geologic contour data for display on top of other images were derived from the digital geologic data. The geologic data were provided by Dr. William Leith of the USGS, based on on-site investigations, treaty exchange, interpretation of satellite photos, and research in the Soviet literature. Topographic information came from the Defense Mapping Agency.

This combination of seismic and non-seismic data provides an environment whereby all available information regarding a particular explosion under investigation is available to the system, in a manner which permits the analyst to effectively integrate it into the best possible yield estimate for the explosion.

3 Overview of System Capabilities

The overall design philosophy which has been followed in the implementation of the YES has been described in Section 2 and in a preceding annual report (Murphy, 1990). In this section, some of the capabilities and functionality of the system will be graphically illustrated through displays of the screens encountered by an analyst in a typical processing session for a selected explosion. For this example, the unclassified data from the Soviet JVE explosion of 14 September 1988 will be analyzed and used to illustrate various features of the system.

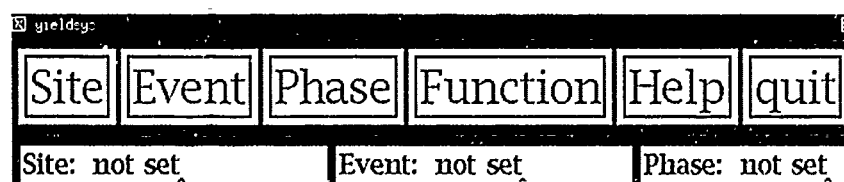
As has been noted previously, a distinguishing characteristic of the YES is that it is completely menu-driven and mouse-activated and requires no keyboard entry by the user. The top level menu providing access to the system is shown in Figure 1 where it can be seen that it consists of six "buttons" which can be used to initiate (SITE, EVENT, PHASE, FUNCTION) or terminate (QUIT) action within the system or to view online information regarding the operating characteristics and parameters of the system (HELP). Selecting any of these buttons with the mouse causes a series of pulldown menus to be activated as illustrated in Figure 2. In this example, the SITE button

has been activated to select the Soviet Shagan River (Balapan) test site, and the EVENT button has been activated to select the JVE explosion which was detonated at that test site on 14 September 1988. Once the test site and event have been selected, the remaining analyst interaction with the system is initiated through the PHASE and FUNCTION buttons. The PHASE button provides the analyst with the capability to choose from among the six different seismic phases listed in Figure 2 for which digital waveform data are currently available on the system. The FUNCTION button provides access to the seven principal computational and analysis modules which permit the analyst to:

- view the seismic data within the context of the available information regarding the specific test location under investigation (*Satellite Image, World Map*)
- interact with the recorded seismic data to process it and extract the various magnitude measures of interest (*Analyst Station, Magnitude Measurement*)

Figure 1.

Main menu structure for YES.



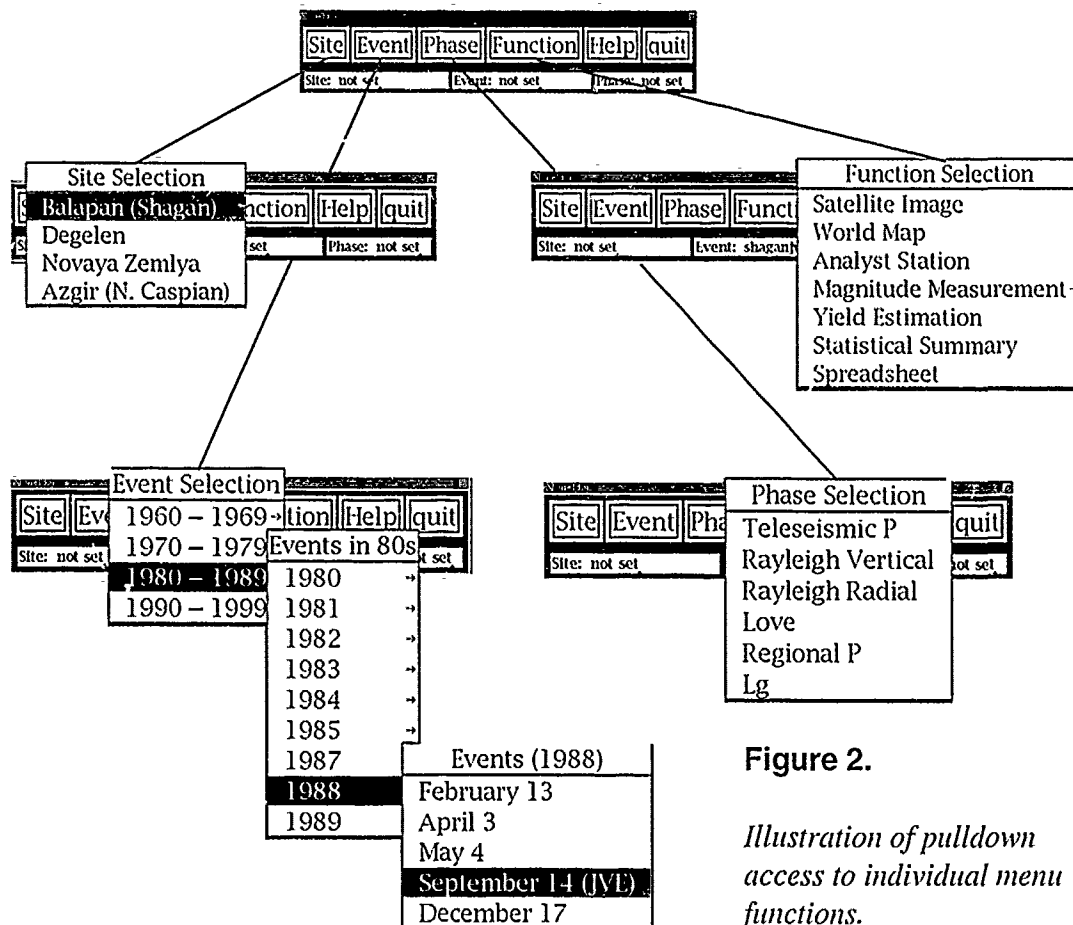


Figure 2.

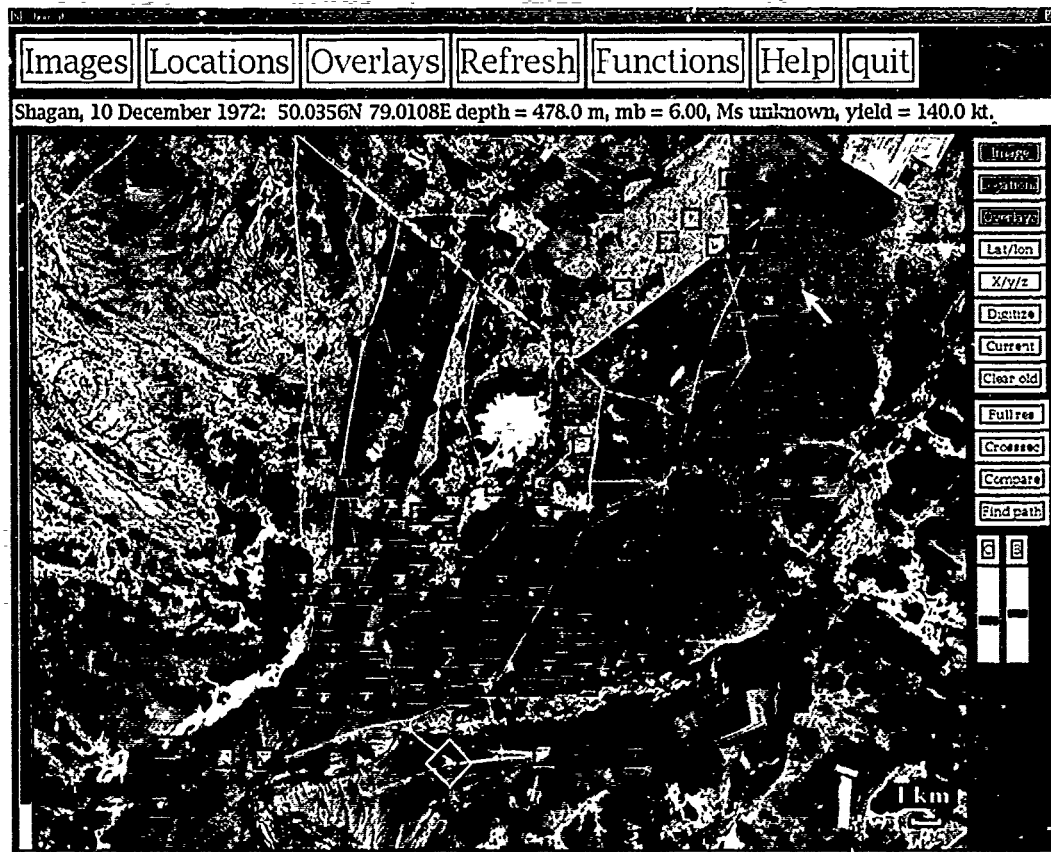
Illustration of pulldown access to individual menu functions.

- formally combine the seismic measures of source size to obtain an optimum measure of explosion yield and quantitative measures of the uncertainty in that estimate (*Yield Estimation*)
- statistically assess the results with respect to any existing treaty thresholds or other yield levels of particular interest (*Statistical Summary, Spreadsheet*).

Having specified a test site and a particular explosion (in this case the JVE event), a typical analysis sequence would begin with the selection of the *Satellite Image* option from the FUNC-

TION menu, which brings to the screen the SPOT satellite image display of the Shagan River test site shown in Figure 3. In this initial display of the test site information interface, the locations of previous explosions at this site are shown as color-coded square overlays, with the current event highlighted by a yellow diamond. In this case, the different colors are used to differentiate those explosions about which the Soviets have published data in the open literature (blue) from those for which only seismic information is available (red). It is important to note that this is not merely a static display, but that in fact the image and the overlays to it are formally tied to an extensive online database of supplementary information. Thus, for

Figure 3. SPOT satellite image of the Shagan River test site with superimposed locations of the historical explosions (squares) and current event (diamond).



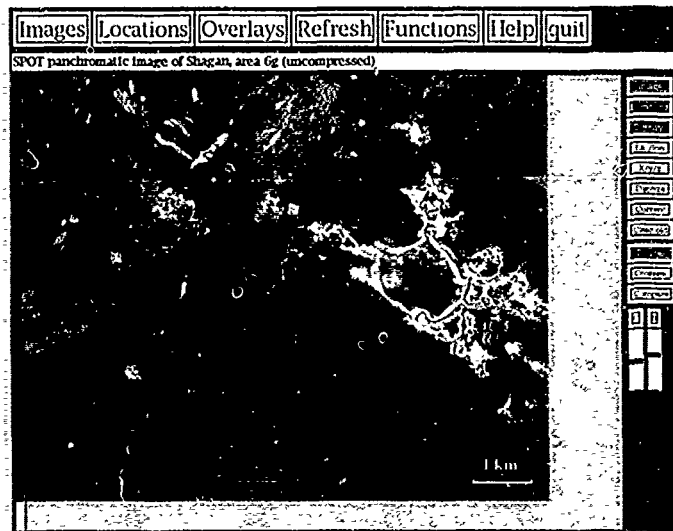
example, in this figure the operator has pointed with the mouse to one of the blue squares (arrow), which has initiated a process by which available information about that event has been extracted from the database and displayed on the information line below the menu buttons, indicating that this explosion was detonated at Shagan on 10 December 1972 at the specified latitude and longitude and that Bocharov *et al.* (1989) have reported the depth as 478m and the yield as 140 kt.

For purposes of display, the satellite image shown in Figure 3 has been compressed to an

effective resolution of about 30m so that the entire test site can be viewed on a single screen. However, the data corresponding to the full 10m resolution of the SPOT image can also be viewed by activating the appropriate button (*Full Res*) on the right hand margin of this display and simply pointing with the mouse to any location on the image. For example, Figure 4 shows the full resolution sub-image corresponding to the location of the cratering explosion of 15 January 1965 which dammed the Shagan River, producing the prominent lake in the southeast quadrant of Figure 3.

Figure 4.

*Full resolution SPOT
satellite image of the region
surrounding the Shagan
River cratering explosion of
15 January 1965.*



Another feature provided by this image display module is the capability to interactively adjust the contrast and brightness using the slider bars located at the bottom of the right hand menu margin.

Figure 5 illustrates this feature by way of a comparison of the nominal display (right) with that resulting from interactively reversing the contrast and decreasing the brightness (left) by reposition-

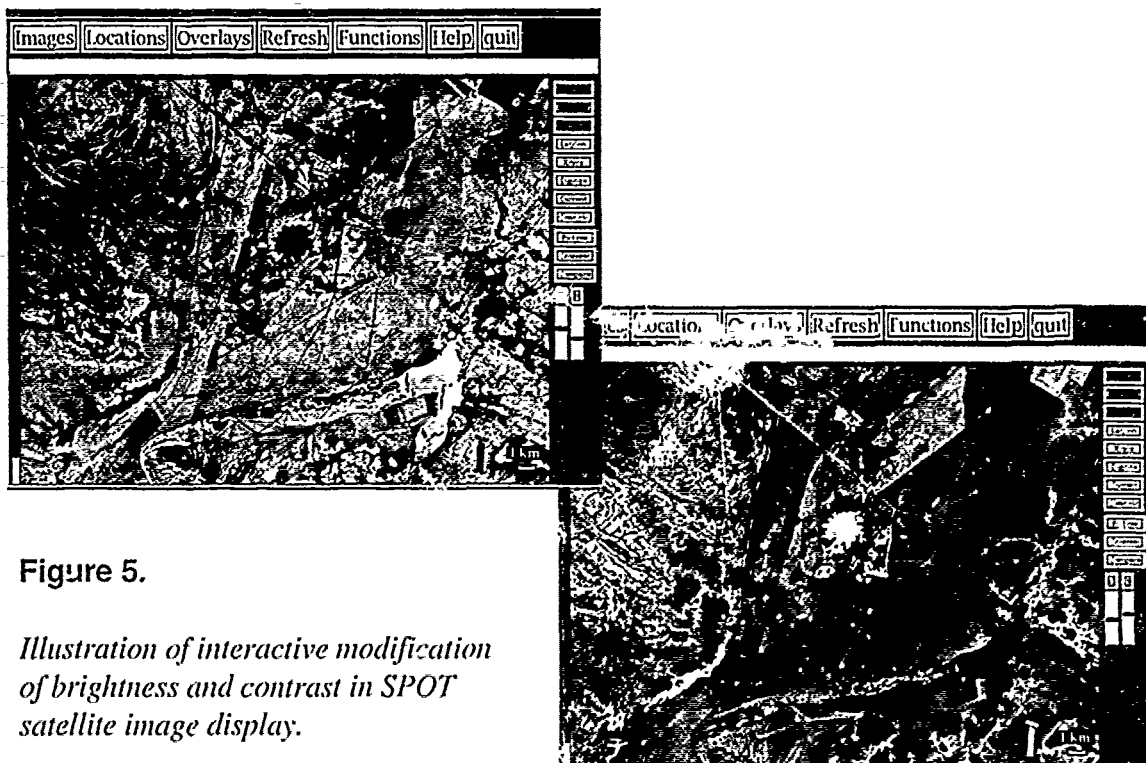
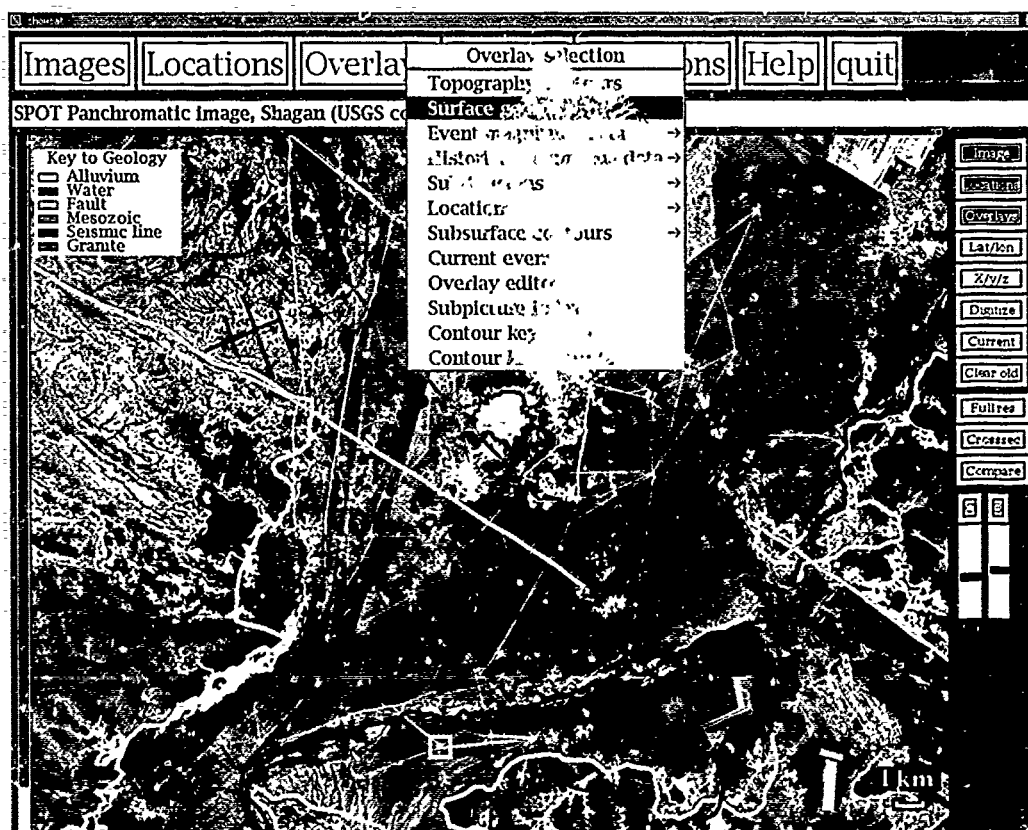


Figure 5.

*Illustration of interactive modification
of brightness and contrast in SPOT
satellite image display.*

Figure 6. SPOT satellite image of the Shagan River test site with superimposed surface geologic map and current event location.



ing these sliders with the mouse. It can be seen that different features are emphasized in these two displays, which facilitates analyst identification of both geologic and man made features.

In addition to the event locations, a number of geologic and topographic databases have been "registered" to this SPOT image and are available for display from the OVERLAYS and IMAGES menus. For example, Figure 6 shows the overlay of Leith's (1989) color-coded, surface geologic map of the area, where the location of the current event (square) is shown in the context of the various exposed geologic units and the trace of the prominent Chinrau fault which intersects this por-

tion of the test site. The Defense Mapping Agency's topographic database for the area is displayed in color-coded image form in Figure 7 together with overlays of the corresponding topography contours and current event location selected from the OVERLAYS menu. Alternately, the variation of surface topography, as well as subsurface geology to a depth of about 1 km, along any specified line across the image can be accessed using the cross-section button (*Crosssec*; on the right hand margin of the image display). This feature is illustrated in Figure 8 where the right hand panel shows the line selected by the analyst by pointing with the mouse to two arbitrary points on the SPOT image

Figure 7.

Color-coded representation of DMA topographic data for the Shagan River test site with superimposed topographic contours and current event location.

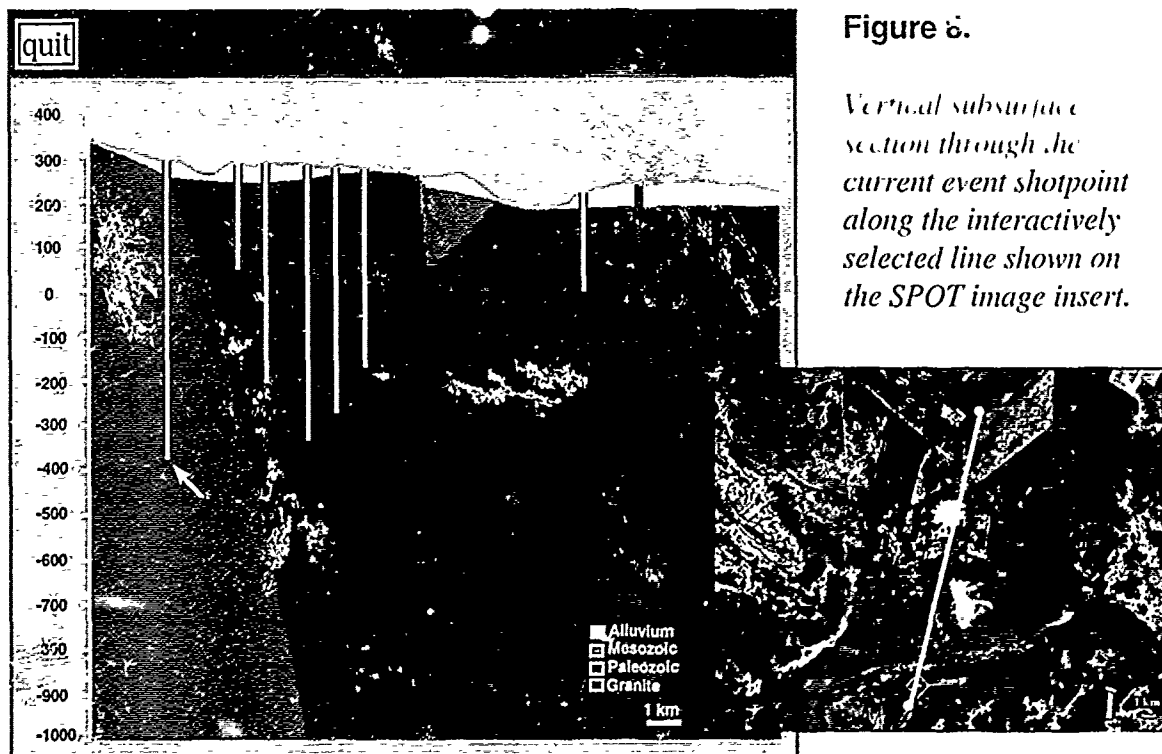
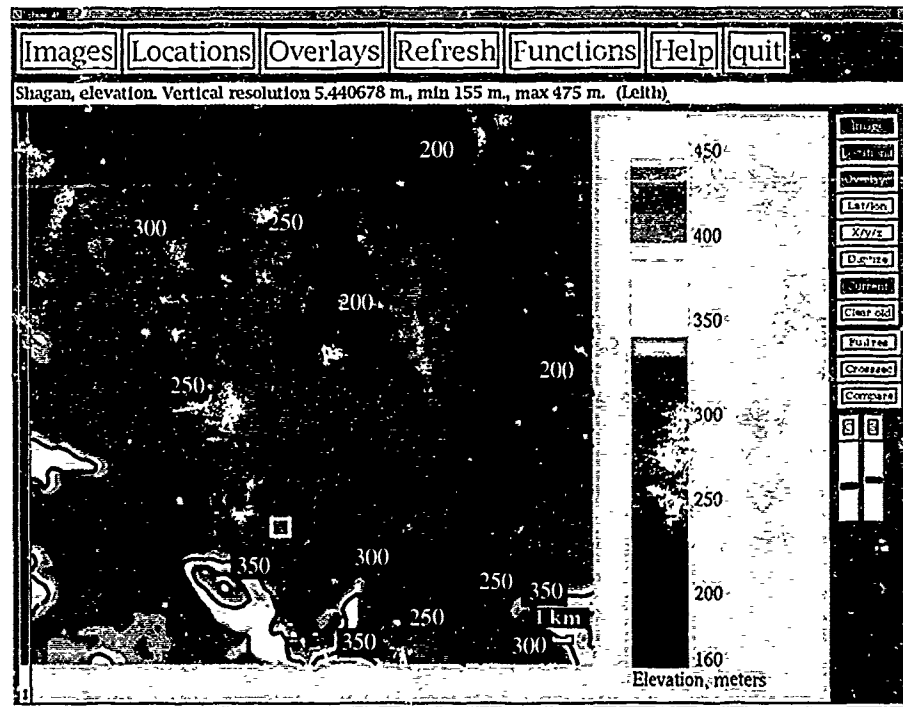


Figure 8.

Vertical subsurface section through the current event shotpoint along the interactively selected line shown on the SPOT image insert.

and the left hand panel shows the resulting vertical section through that line which was automatically produced by the system, together with the locations and approximate depths of penetration of explosion emplacement holes encountered along that line. As with the surface topography, the variation in the depth to any selected geologic interface can also be exhibited in image form, as illustrated for the granite surface in Figure 9 where, once again, the corresponding depth contours and location of the current event have been overlaid for reference purposes. It is immediately evident from this presentation that, unlike the current JVE event,

most previous explosions at this test site have not been detonated in granite in that the granite surface throughout much of this region lies uniformly below typical explosion emplacement depths.

Having completed an initial review of the available information regarding the explosion test environment, the analyst can next proceed to an examination of the corresponding recorded seismic data. As an initial step, an overview of the locations of stations for which data from the selected explosion are available on the system can be obtained by selecting the *World Map* option from the FUNCTIONS menu. The resulting displays

Figure 9. *Color-coded representation of depth to the top of the granite surface beneath the Shagan River test site with superimposed depth contours and current event location.*

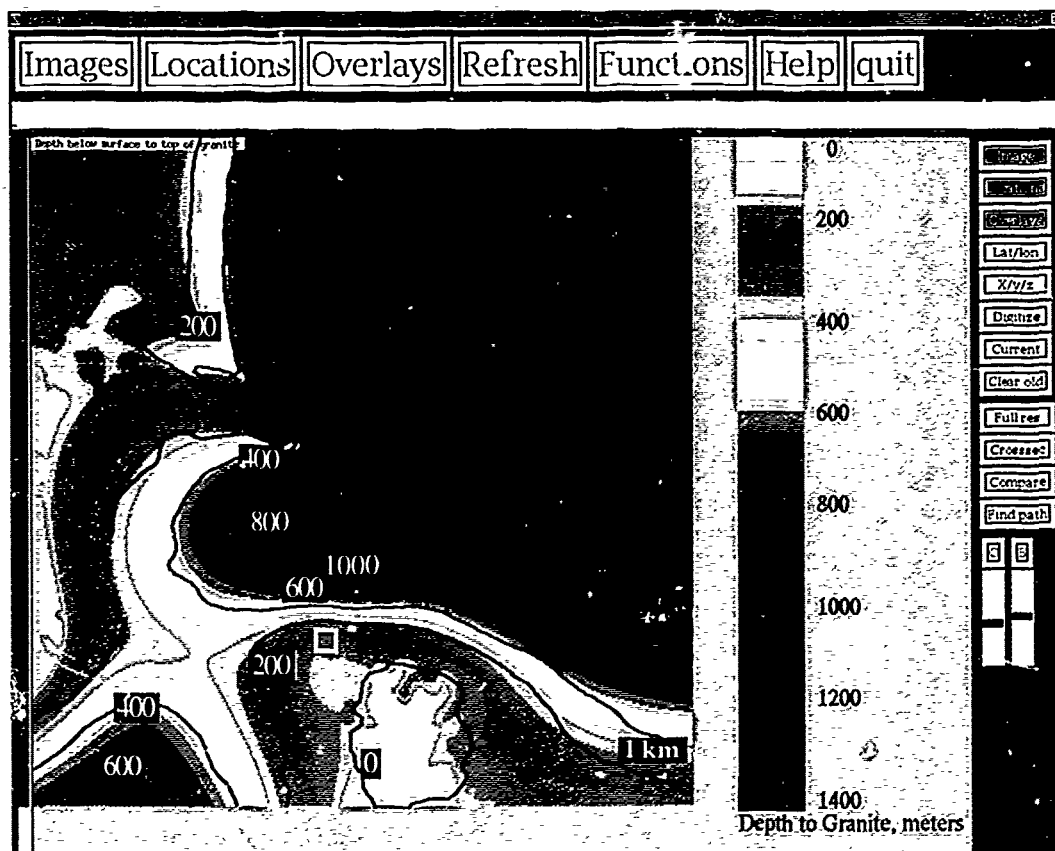
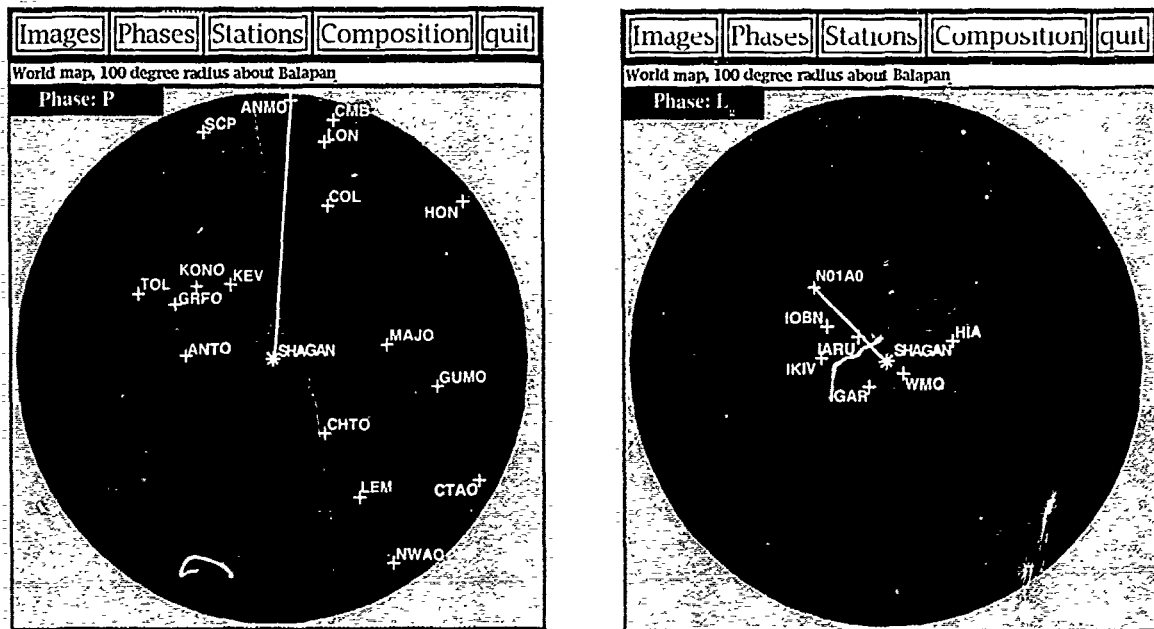


Figure 10. World map projections ($\Delta < 100^\circ$) showing locations of stations for which digital teleseismic P (left) and L_g (right) data are available for the current event.

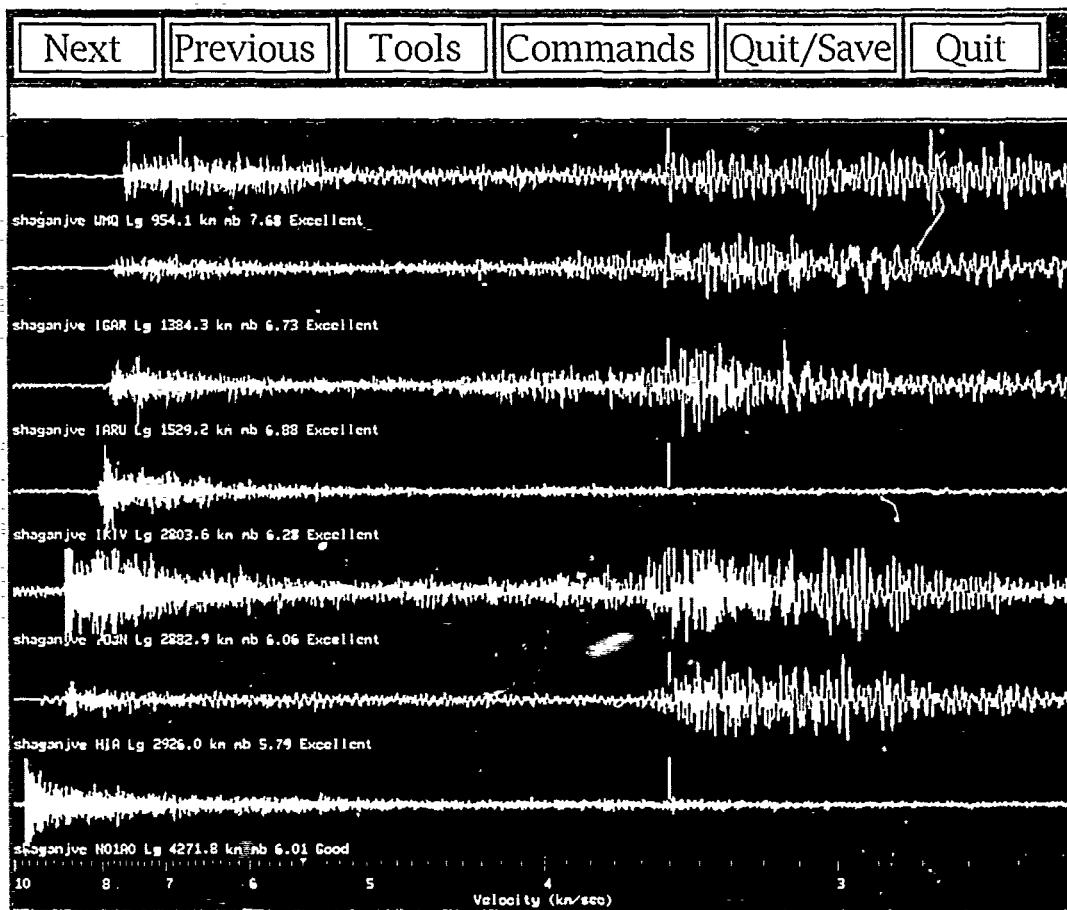


for the JVE teleseismic P and regional L_g phases are shown in Figure 10, plotted on azimuthal equidistant projections of the globe ($\Delta < 100^\circ$) centered on the Shagan River test site. As illustrated here, a menu item (STATIONS) within this module provides the user with the capability to select any one of these recording stations from a list and subsequently cause a straight line to be drawn on the screen between the source and the receiver. In this transformation, the straight line corresponds to the great circle path and thus provides the analyst with a view of the surface projection of the propagation path followed by the main energy groups between these two points.

The seismic data themselves can be accessed by returning to the main menu (Figure 2)

and sequentially selecting a seismic phase from the PHASE menu and *Analyst Station* from the FUNCTION menu. Thus, for example, specifying the phase L_g in this manner automatically initiates a process by which the L_g recordings from the JVE explosion are extracted from the online database of digital waveform data and displayed on the screen in the format shown in Figure 11. In this and subsequent seismogram displays, the stations are ordered by increasing epicentral distance and, for the L_g and surface waves, the data are plotted as a function of group velocity. It can be seen in this figure that the traces are marked by a vertical line at a group velocity of 3.5 km/sec, indicating the nominal expected onset time of the L_g phase. This display permits the analyst to quickly assess the

Figure 11. Analyst station display of vertical-component L_g signals for the current event.



quality of the data and identify any prominent characteristics. Thus, for example, it can be seen from Figure 11 that the L_g signals are relatively weak at the IRIS station KIV (IKIV) and at NORSAR (N01A0), consistent with the expected effects of propagation across the Caspian Sea (KIV) and along the complex, far-regional path to Norway.

Having verified that the available L_g data are suitable for further processing, the analyst can proceed to magnitude estimation by selecting

the *Magnitude Measurement* option from the FUNCTION menu as illustrated in Figure 12. Selecting *RMS L_g* from this list of five currently available magnitude measures initiates a series of

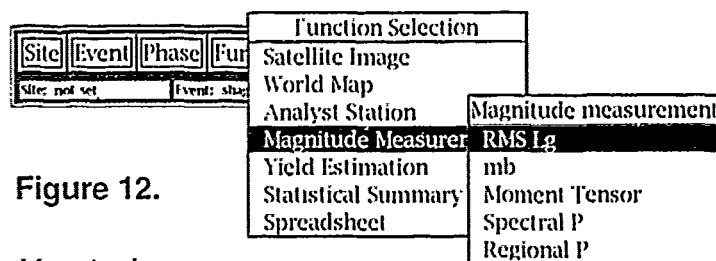


Figure 12.

Magnitude measurement menu.

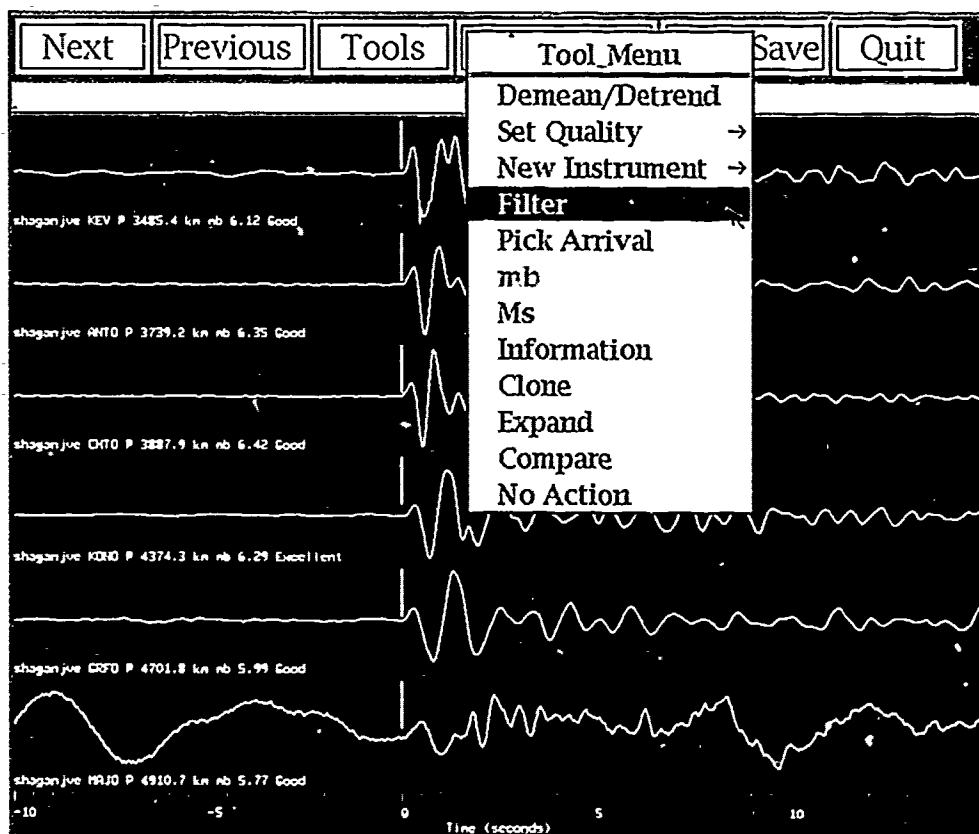
operations by which the L_g waveforms recorded from the JVE event are automatically processed using algorithms described by Ringdal (1983) to obtain single-station and network-averaged measures of the L_g magnitude, M_{Lg} . Since this processing takes some time to accomplish, it is run in the background, thereby permitting the analyst to move on to other tasks while it is being completed. In the present example, the analyst has selected *Teleseismic P* from the PHASE menu and *Analyst Station* from the FUNCTION menu, resulting in the waveform display shown in Figure 13. The P wave seismograms are plotted here as a function of reduced time, extending from 10 seconds before to 15 seconds after the signal onset

time which is denoted by the vertical line segments. Generally, there are more recordings than can be displayed on a single screen in this format and, in such cases, the analyst can readily page forward and backward through these multiple screens using the NEXT and PREVIOUS menu buttons at the top of the analyst station display.

An extensive set of signal processing and analysis capabilities has been assembled within the analyst station module, as indicated by the TOOLS menu display in Figure 13. These tools permit the analyst to:

- assign waveform quality (*Set Quality*),
- redefine arrival times (*Pick Arrival*),

Figure 13. *Analyst station display of selected vertical-component teleseismic P wave signals for the current event.*



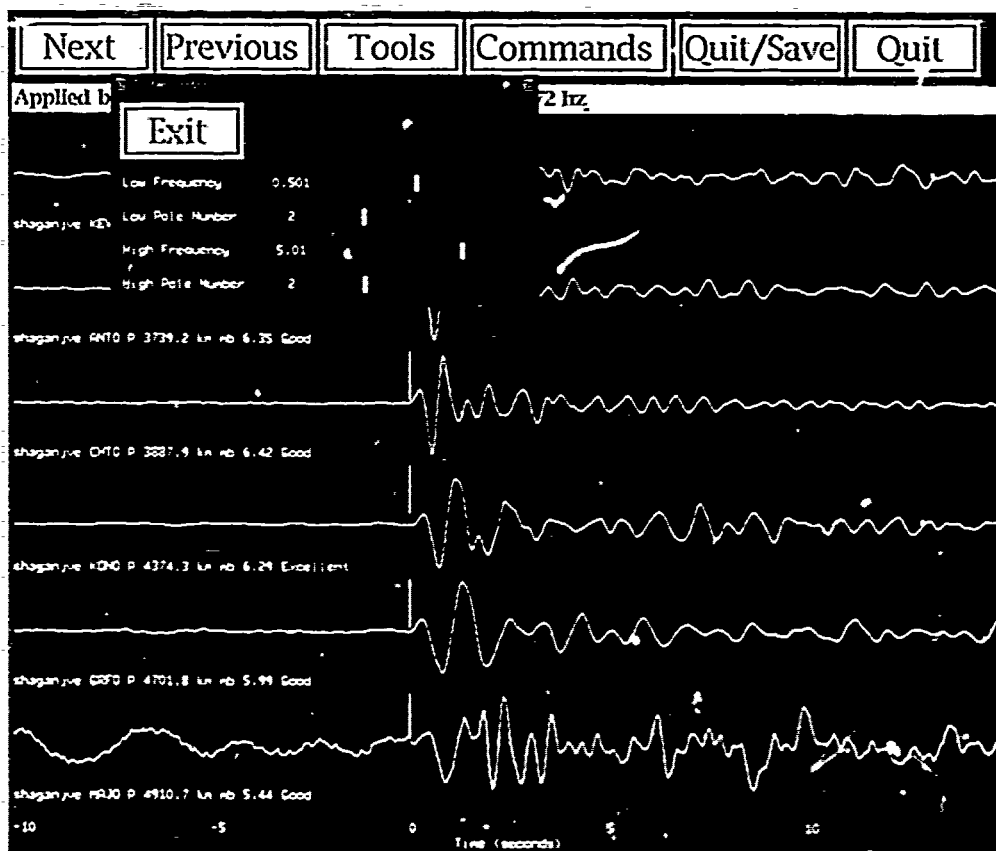
- measure amplitudes and periods (*Expand, mb, Ms*),
- filter the data (*Demean/Detrend, Filter*),
- normalize to a common instrument response (*New Instrument*) and
- compare a selected waveform with waveforms recorded at that station from previous explosions (*Compare, Clone*).

Thus, for example, it can be seen from Figure 13 that the P wave signal recorded at station MAJO in Japan (bottom trace) is obscured by microseismic noise lying outside the signal pass-band. Selecting *Filter* from the TOOLS menu

causes the interactive filter interface to be displayed as shown in Figure 14, where the analyst has used the mouse to adjust the slider bars to define low and high frequency cutoffs of 0.5 and 5.0 Hz, respectively, and to specify a second order roll-off outside that band by setting the corresponding pole numbers to 2. Subsequent selection of any trace with the mouse causes this filter to be automatically applied and the result displayed, as shown here for station MAJO.

Application of the *Compare* function from the TOOLS menu provides another illustration of the powerful capability for interactive analysis which is available in the analyst station. For

Figure 14. *Example of the specification and subsequent application of a bandpass filter to the data of Figure 13.*



example, by sequentially selecting this function and the station KONO waveform from Figure 14, a search through the database is automatically initiated to identify all other available P waveforms recorded at that station from previous Shagan River explosions. Generally, not all of the explosions identified by this search are of equal importance for comparative purposes and selection of a meaningful subset is facilitated by examining their locations in the context of the SPOT image test site information interface, as indicated in Figure 15. Using this interface, the analyst can interactively select specific events with the mouse, as indicated

here by the diamond overlays, on the basis of proximity to the current event or some other criterion, and display the corresponding P waveforms in a time expanded analyst station mode such as that of Figure 16. Here the current JVE event recording is shown at the top of the figure and the waveforms from the selected comparison events are displayed beneath it in the order in which they were selected. Also illustrated in this figure is the use of the *Clone* feature from the TOOLS menu which permits the operator to select any trace on the screen with the mouse (in this case the JVE recording), create a color-coded (red) copy and

Figure 15. *SPOT locations of Shagan River explosions recorded at station KONO in Norway. The diamond symbols denote those events selected for comparative analysis.*

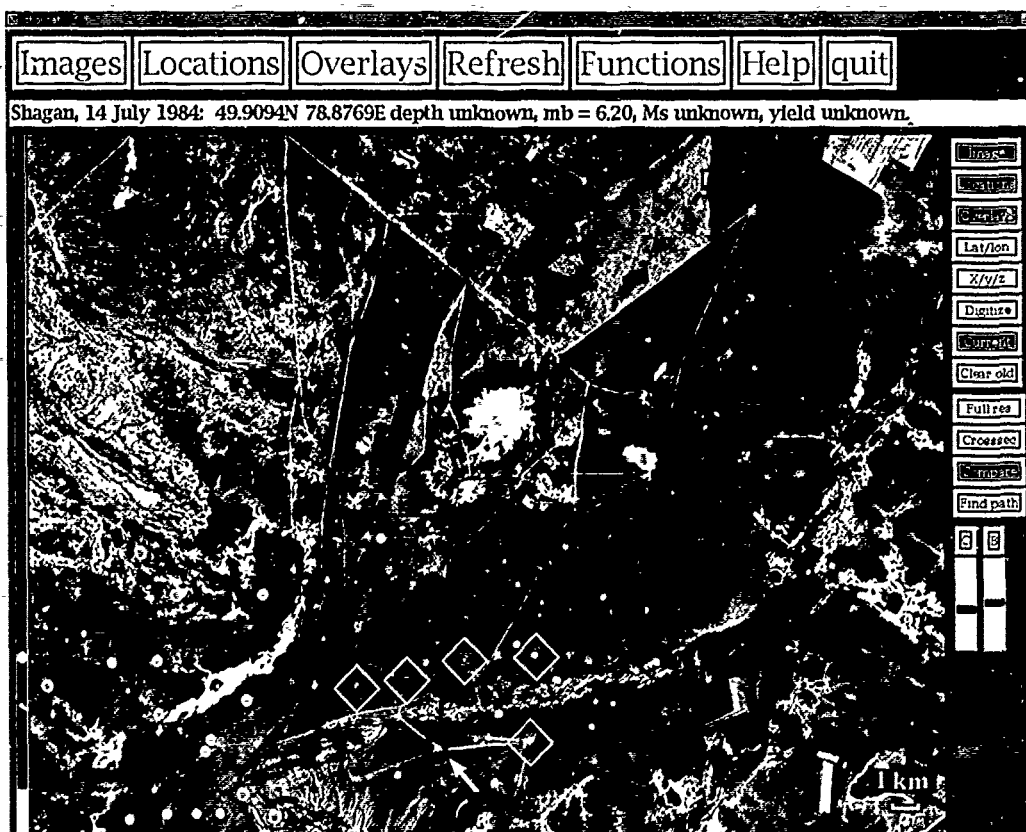
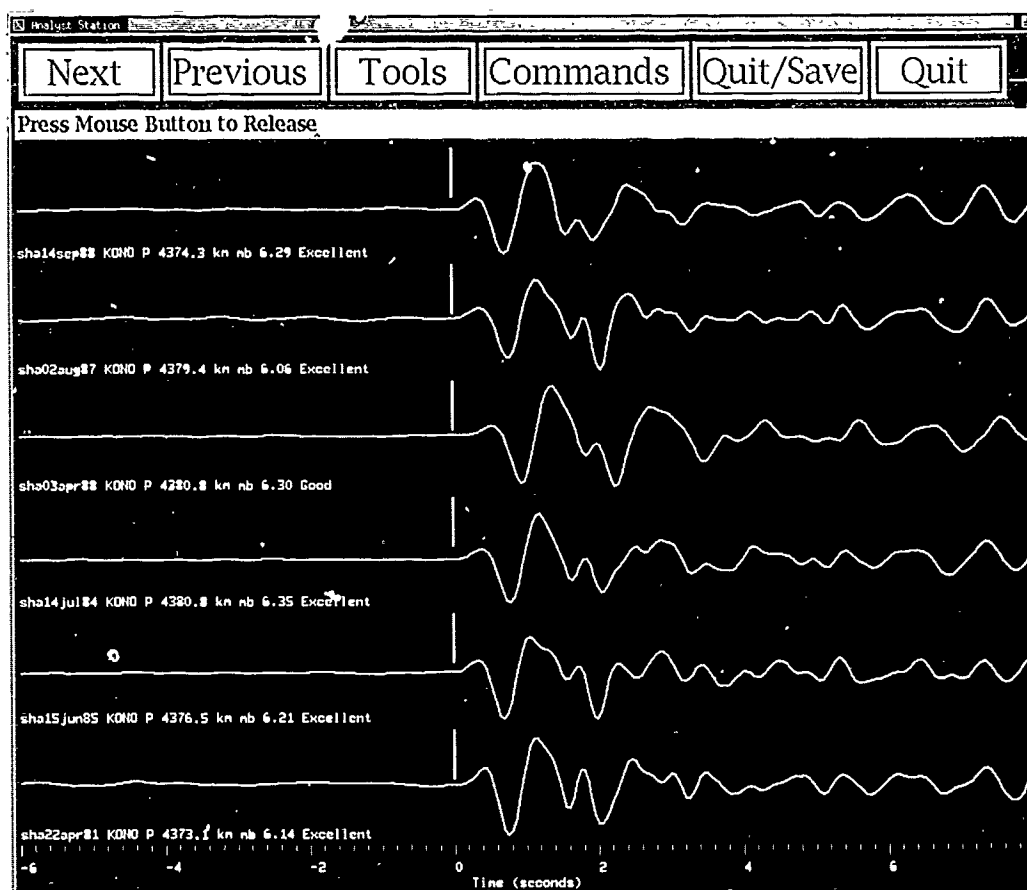


Figure 16. Comparison of the P wave signal recorded at station KONO from the current event (top and red) with the signals recorded at that station from the selected events of Figure 15.



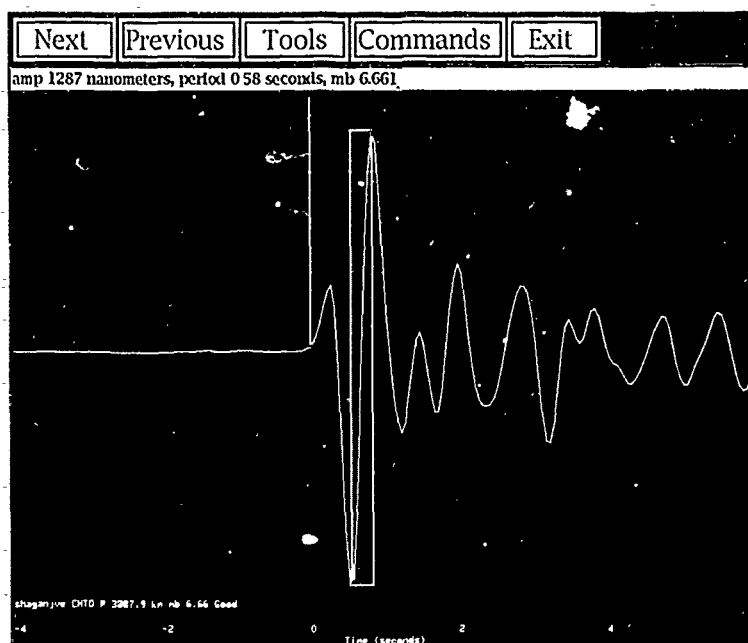
drag it to any other location on the screen to conduct detailed waveform comparisons. This capability permits the analyst to quickly assess the consistency of the current observation with past experience and, in this case, to conclude that the JVE recording at KONO is quite consistent with previous observations at that station from other explosions located in that area of the test site.

Once the initial waveform review has been completed, the analyst can proceed to magnitude estimation using the *Expand* and *mb* functions from the TOOLS menu. By sequentially selecting *Expand* and any waveform from the analyst sta-

tion display, a magnified reproduction of that waveform is produced as shown in Figure 17. Then, by employing the *mb* function, the mouse can be used to position a rectangle so as to define the peak-to-peak amplitude and half period of the selected cycle of motion as shown in this figure. After this process has been repeated for each usable trace, the resulting amplitudes are input to the *mb* estimation module using the *Magnitude Measurement* menu of Figure 12 where they are converted to ground motion, corrected for epicentral distance and station effects and logarithmically averaged to obtain a network-averaged *mb* value and associ-

Figure 17.

Illustration of the interactive determination of the amplitude and period values used to define single station m_b values.



ated uncertainty. The resulting individual station m_b values for the current JVE explosion are displayed in Figure 18, together with the estimated network-averaged value of 6.012. This display module also provides the capability for the analyst to interactively eliminate questionable data points and then to recalculate the network average using the ADD/DELETE and RECALC menu buttons shown at the top of the figure. This process can be continued until a final stable m_b estimate is obtained, at which time it is written to the database using the designated SAVE menu button.

Note from Figure 18 that at this point the system has notified

the analyst that the RMS L_g magnitude estimation has been completed, as indicated by the icon in the upper left hand corner of this display. Selecting this icon with the mouse produces the display of individual station and network-averaged M_{Lg} values shown in Figure 19. It can be seen from this figure that the estimated network-averaged M_{Lg}

Figure 18.

Comparison of individual station and network-averaged m_b magnitudes determined for the current event.

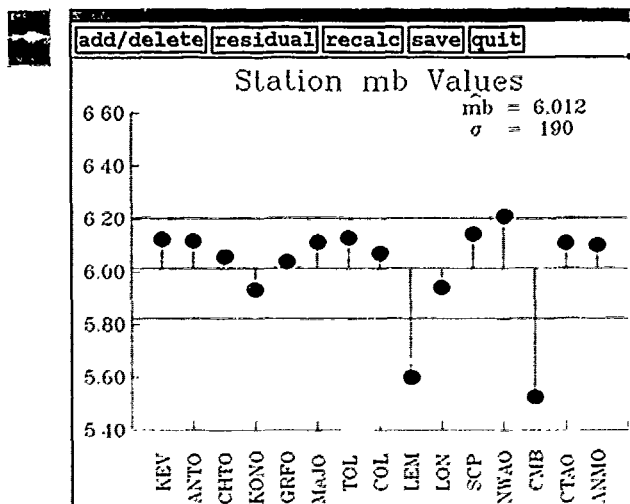
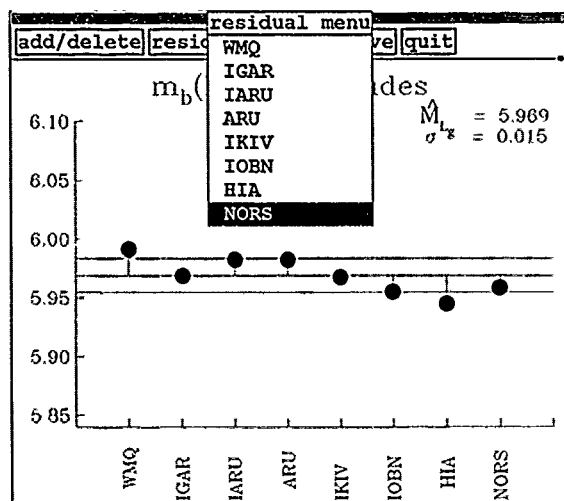


Figure 19.

Comparison of individual station and network-averaged M_{Lg} magnitudes determined for the current event.



value of 5.969 is somewhat lower than the corresponding m_b value of 6.012 of Figure 18, and it would be natural for the analyst to question whether there is any significance to this difference. This issue can be addressed by selecting a representative station (e.g., NORS) from the RESIDUAL menu

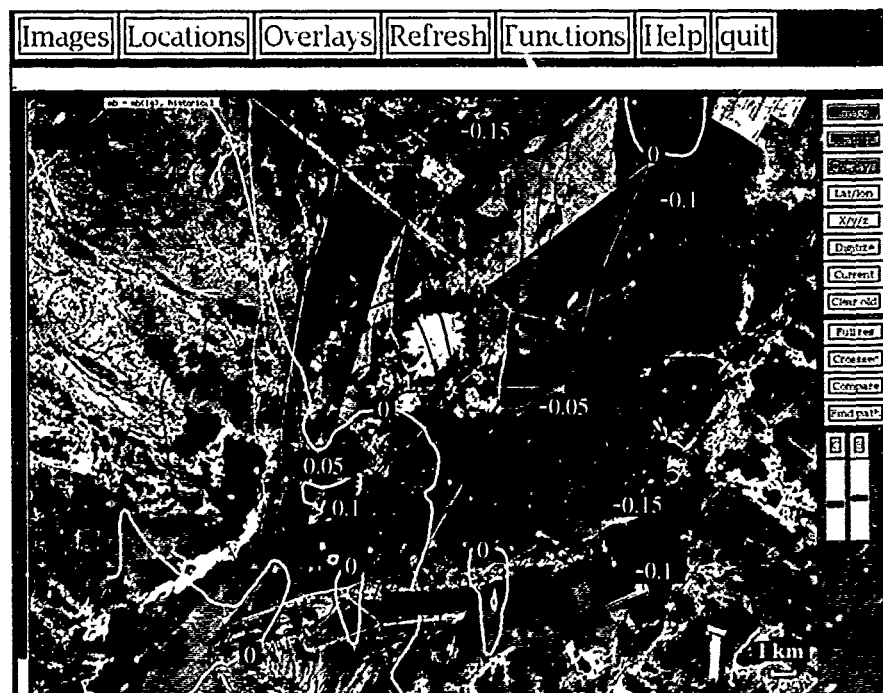
display that while this magnitude difference is typically negative in the northeast quadrant of the test site (by as much as 0.15 magnitude units), it is generally positive in the vicinity of the current JVE event location, with an average value close to the observed value of 0.043. Thus, this capability

on this display and returning to the SPOT image test site information interface to overlay the quantity $m_b - M_{Lg}(NORS)$ at the current event location as in Figure 20, where contours of this quantity derived from results of previous explosions have also been overlaid for reference purposes.

It can be seen from this

Figure 20.

Comparison of the observed value of $m_b - M_{Lg}(NORSAR)$ for the current event with contours representing observed variation of that parameter for previous events.

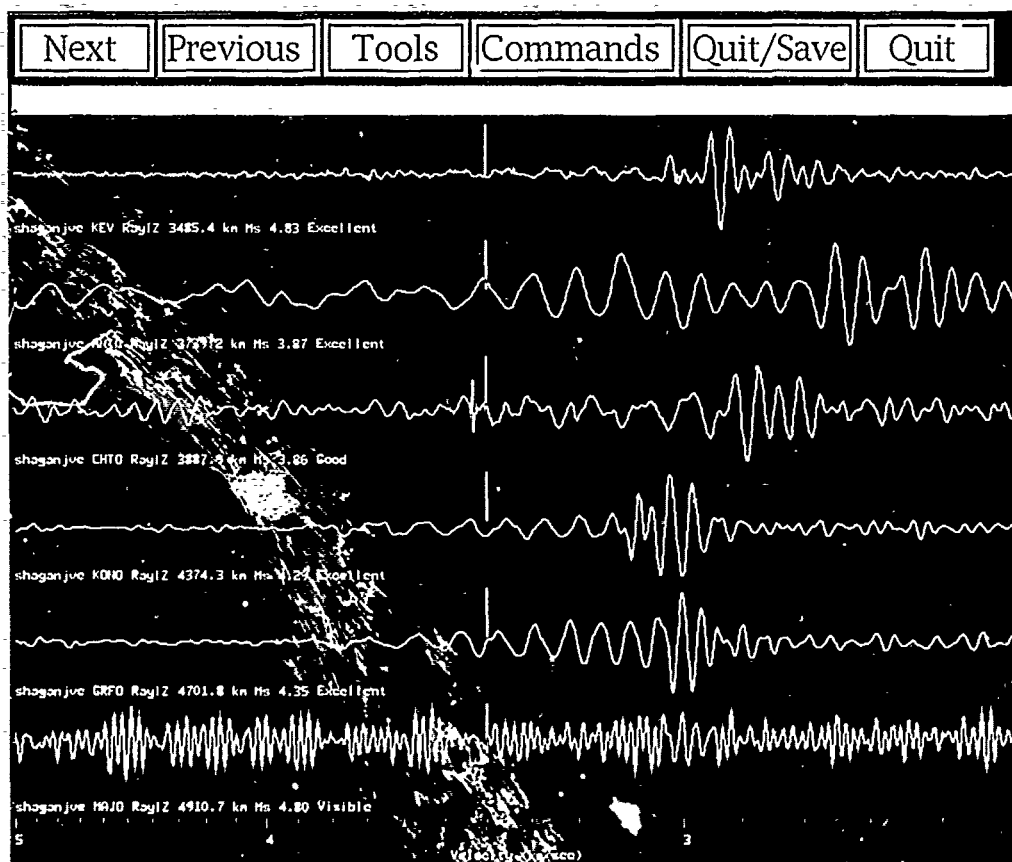


permits the analyst to quickly conclude that the current result is entirely consistent with previous experience in this area of the test site.

The long-period surface wave data can be accessed in the same manner as the L_g and P phase data described above, resulting in analyst station displays such as that shown in Figure 21 for the vertical component Rayleigh wave phase. It can be seen from this example that, although these traces are aligned according to a common group velocity scale, the surface wave signals are quite variable and difficult to correlate from trace to trace. This is at least partially due to the fact that the response

characteristics of the long-period instruments used to record these data vary significantly between stations. Thus, for example, the station MAJO trace shown at the bottom of this figure was recorded through a relatively broadband system, with the result that the long-period signals of principal interest are obscured by higher frequency arrivals. In order to provide a common basis for comparison, the TOOLS menu includes a function (*New Instrument*) which permits the analyst to transform the data to that which would have been observed if the same instrumentation had been employed at each station. This feature is graphi-

Figure 21. Analyst station display of selected long-period Rayleigh wave signals for the current event.



cally illustrated in Figure 22 where the analyst has selected the nominal SRO long-period response and converted all of the traces in this display to that response by simply designating them with the mouse. It is evident from this example that such a capability greatly facilitates quantitative comparisons and evaluation of data.

Once the available long-period Rayleigh and Love wave data have been previewed, the analyst can return to the *Magnitude Measurement* menu of Figure 12 and select *Moment Tensor*, thereby initiating a process by which the observed long-period data are formally inverted to

obtain a surface wave measure of seismic magnitude. While this computationally intensive process is running in the background, the analyst next selects *Spectral P* from this same menu and proceeds with an interactive determination of the network-averaged P wave spectrum corresponding to the current event. The spectrum estimated in this process can be inverted to obtain either an equivalent spectral magnitude or a direct, model-based yield estimate (Murphy, 1989), and Figure 23 shows the menu structure for the latter option, where it is indicated that the Mueller/Murphy granite (M/M Granite) source model has been

Figure 22. Example of the specification and subsequent application of the instrument response normalization feature to the data of Figure 21.

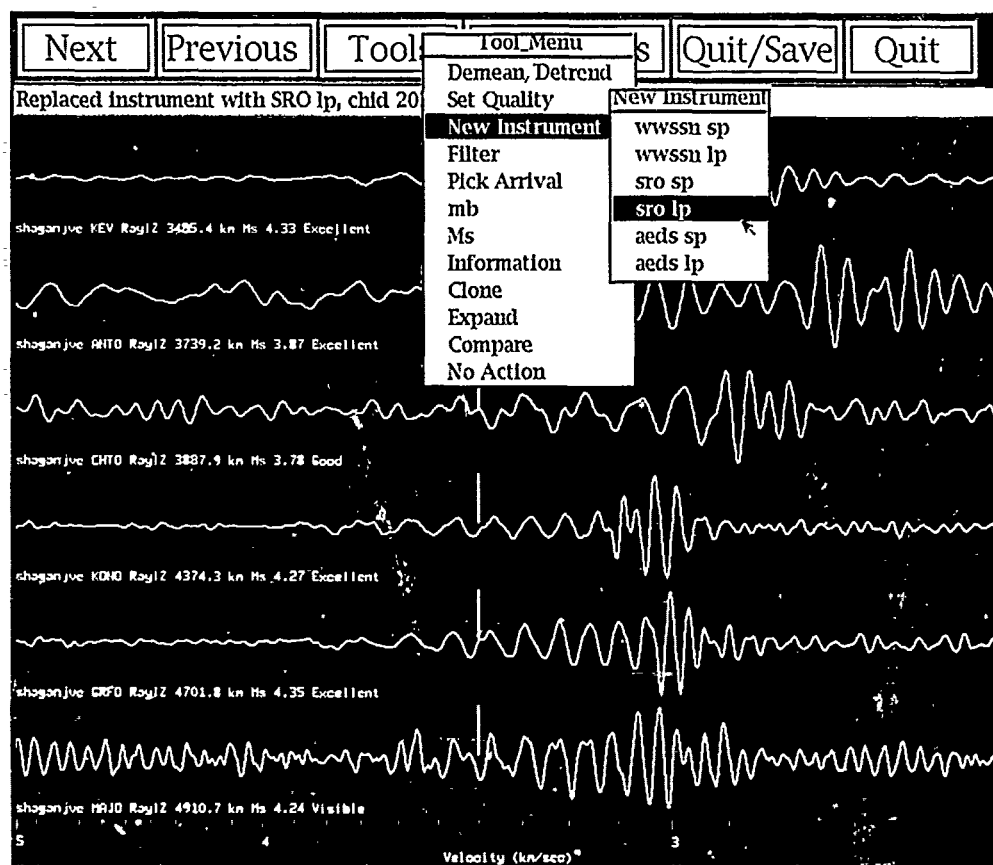
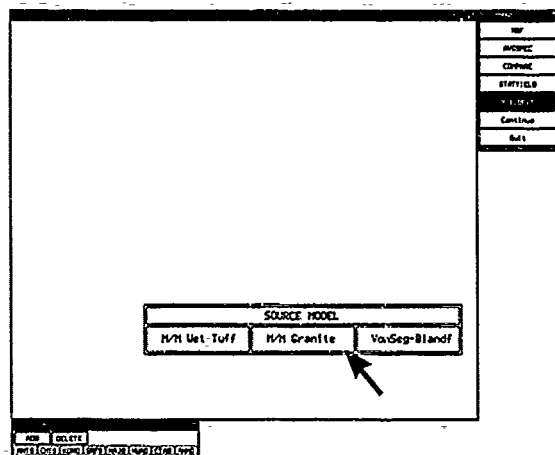


Figure 23. *Menu options for the estimation of network-averaged P wave spectra.*



selected for the current JVE event. The resulting automatic fit to the attenuation-corrected, observed spectrum is shown in Figure 24 where it is indicated that a theoretical spectrum corresponding to a yield (W) of 119 kt, a pP - P delay time (t_0) of 0.82 seconds and a pP/P amplitude ratio (A) of 0.17 provides the best overall fit to the data. Alternately, the analyst can elect to interactively change these automatically determined model parameters using the plus and minus buttons located in the box in the upper right corner of this display, to explore solutions corresponding to goodness of fit criteria not incorporated in the automatic algorithm.

The icon appearing in the upper left corner of Figure 24 indicates that the surface wave moment tensor inversion processing has now been

Figure 24. *Comparison of normalized observed and best-fitting theoretical network-averaged P wave spectra for the current event.*

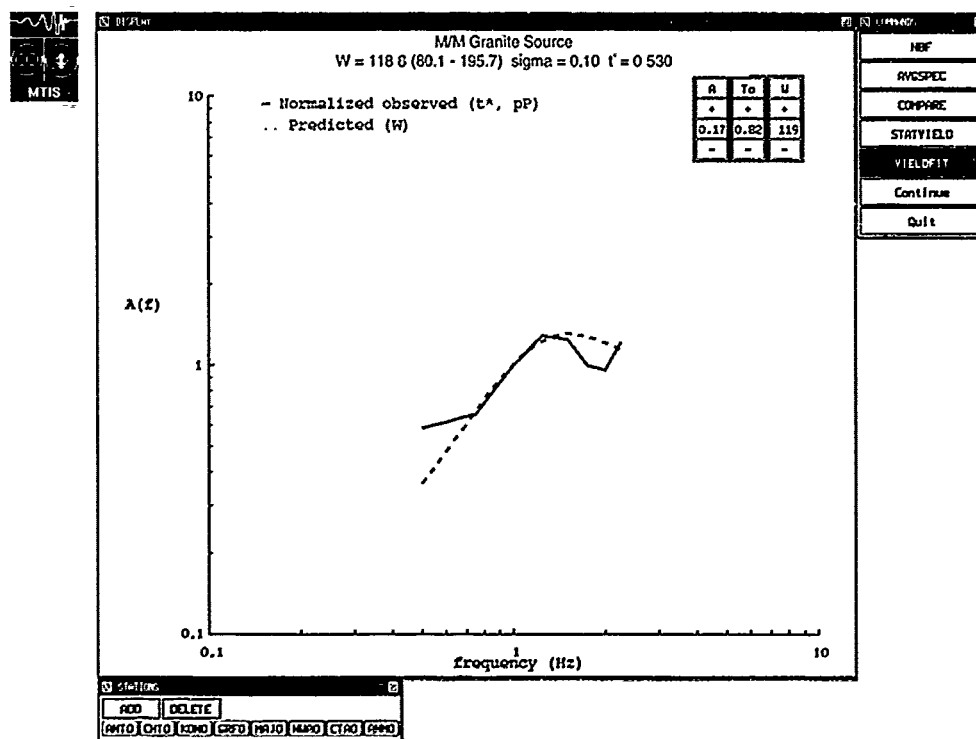
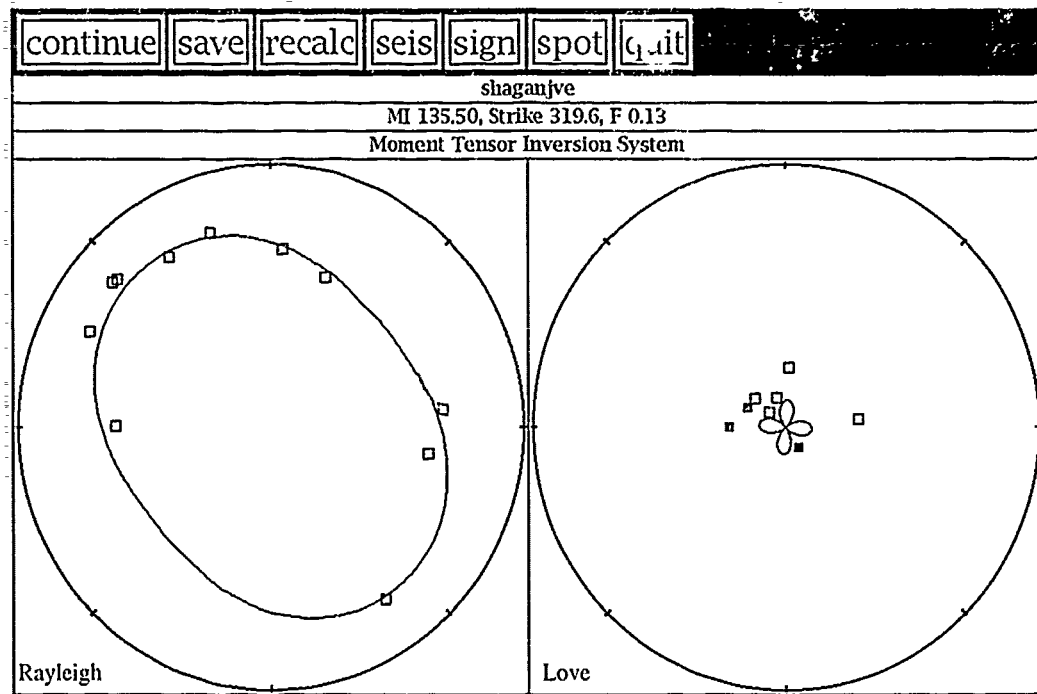


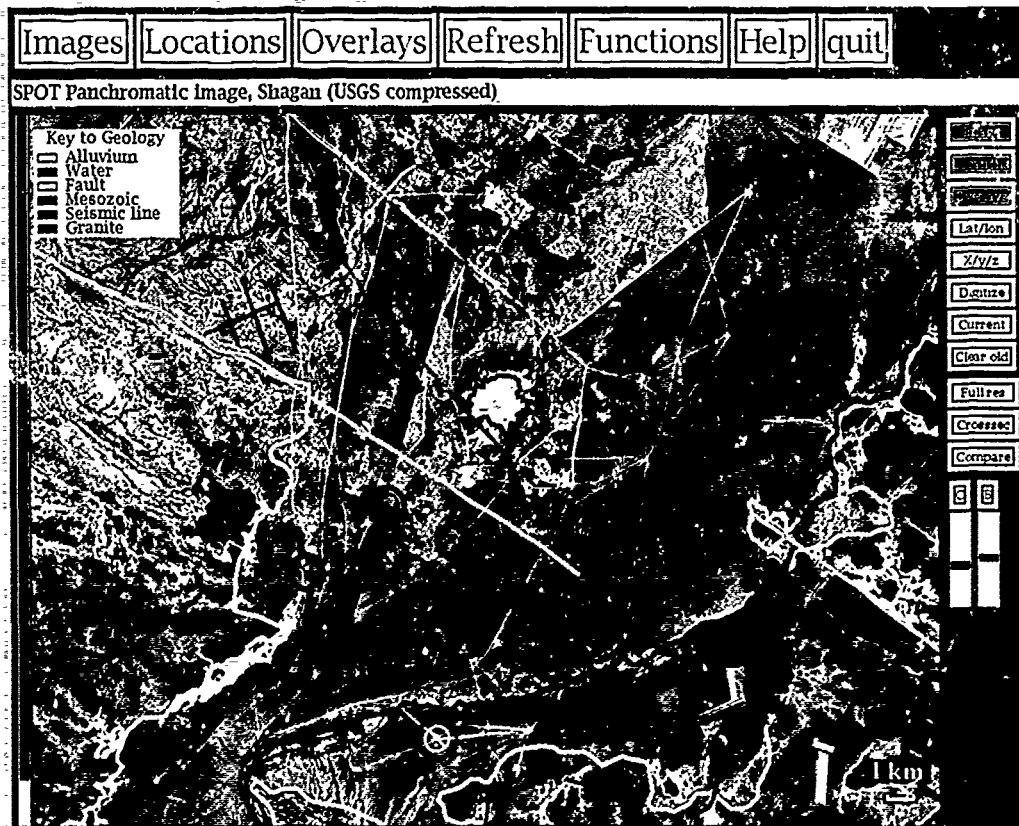
Figure 25. Comparison of the inferred surface wave moment tensor solution for the current event with the corresponding path normalized, observed Rayleigh (left) and Love (right) wave amplitude data.



completed, and selecting it with the mouse produces the graphical solution summary of Figure 25 where the model fits to the Rayleigh (left) and Love (right) wave data corresponding to a tectonic release F factor of 0.13 are displayed. It is informative to examine this solution in the context of other available information regarding the test environment. This can be accomplished by returning once again to the SPOT image test site information interface and successively overlaying the current and historical moment tensor solutions, as well as the map of surface geologic features, as shown in Figure 26. In this display, the concentric circles represent the moment tensor solutions where, for the historical events, the ratio of the diameters of the red-to-blue circles is equal to the inferred tectonic release F factors and the line segments

interior to the circles are parallel to the associated strike of the tectonic component. The solution for the current (JVE) event is differentiated here by an alternate color scheme in which yellow and light blue circles replace red and blue, respectively. It can be seen from this display that the solution for the current event is quite consistent with those previously determined for nearby historical events. Moreover, it is evident that the inferred strikes of the tectonic releases triggered by these explosions are parallel or subparallel to that of the mapped Chinrau fault. Thus, by using the test site information interface, the analyst is able to quickly verify that the surface wave moment tensor solution which was obtained for the current event is consistent with both the solutions from previous nearby explosions and with the regional tectonic environ-

Figure 26. Comparison of the surface wave moment tensor solution for the current event (yellow and light blue concentric circles) with those for nearby Shagan River explosions (red and dark blue concentric circles) and with the surface geologic map of the area.



ment in which the test was conducted.

Having determined the various seismic measures of source size (including a regional P_n magnitude not discussed above), the analyst can proceed to estimate the corresponding explosion yield and the associated uncertainty in that estimate by selecting the *Yield Estimation* feature from the **FUNCTION** menu of Figure 2. This yield estimation module provides an estimate of unified yield based on multiple magnitude measures and associated "extremal confidence limits" corresponding to different sets of constraints specified by the analyst. The confidence limits are obtained

as the solution of a nonlinear programming problem in which estimates of yield for a training set of explosions are minimized and maximized over the space of admissible parameters (Rodi, 1989, Rodi and Murphy, 1990). Input to this model consists of multiple network-averaged magnitudes for the current event and a nominal m_b /yield relation based on some combination of data analysis and expert opinion, which for explosions at the Shagan River test site is taken to be (Murphy, 1990).

$$m_b = 4.45 + 0.75 \log W$$

The current module can provide estimates corresponding to five different sets of constraints, parameterized by the uncertainty in the average value of m_b at 100 kt ($m_b(100)$), the uncertainty in the slope (b) of the m_b /yield relation and the upper bound on the absolute value of the correlation coefficients amongst the yield estimation errors for the individual magnitudes (max P). The menu for the yield estimation module is shown in Figure 27 together with sample output corresponding to the application of Models 1 and 3 to the magnitude data for the current JVE event. In these displays, the resulting unified yield estimates (W) and associated upper bound uncertainty factors (F) are shown, together with the yield estimates obtained from the individual magnitude values. Note that the P_n yield value is shown here as an open circle to denote the fact that it was not used in the formal computation of W and F due to the fact that an

adequate training set of previous values does not currently exist for that magnitude measure. It can be seen that for these two cases, the unified yield estimate is about 121 kt and the uncertainty bounds range from a factor of 1.96 for the case (Model 1) in which $m_b(100)$ is specified as 5.95 ± 0.05 , to a factor of 1.66 for the case (Model 3) in which $m_b(100)$ is given as exactly 5.95. In Figure 28, the Model 1 solution from Figure 27 (top) is compared with the result of rerunning Model 1 without the surface wave moment tensor magnitude (i.e., by using the slider bars at the bottom of the menu box to assign a weight of zero to $W(M_0)$). It can be seen that this modification results in a significant reduction of the F factor from 1.96 to 1.55, reflecting the relatively uncertain yield estimation capability of the surface wave moment as determined from the analysis of the training set of multiple magnitude data.

Figure 27.

Menu and sample output for the unified yield estimation module.

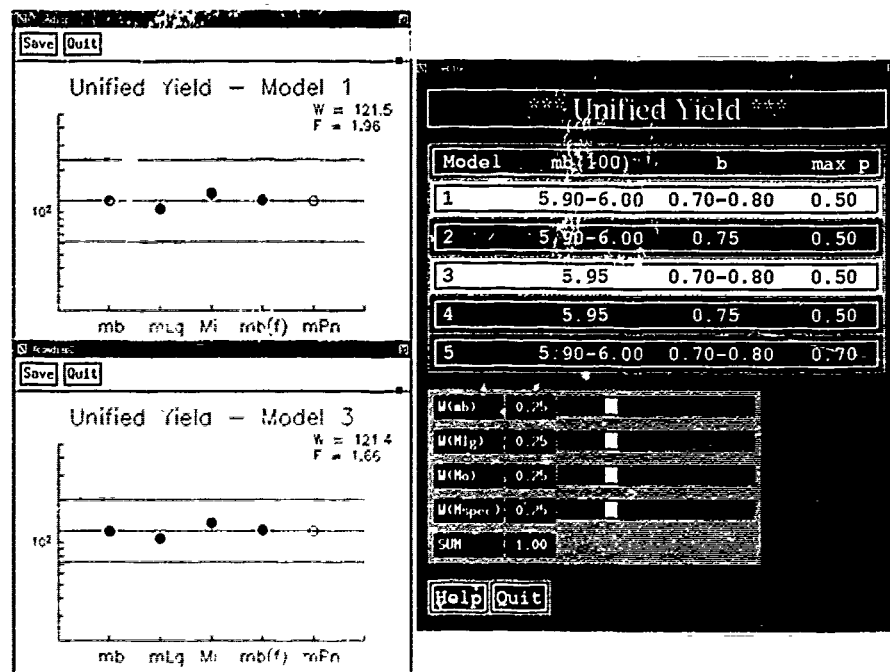
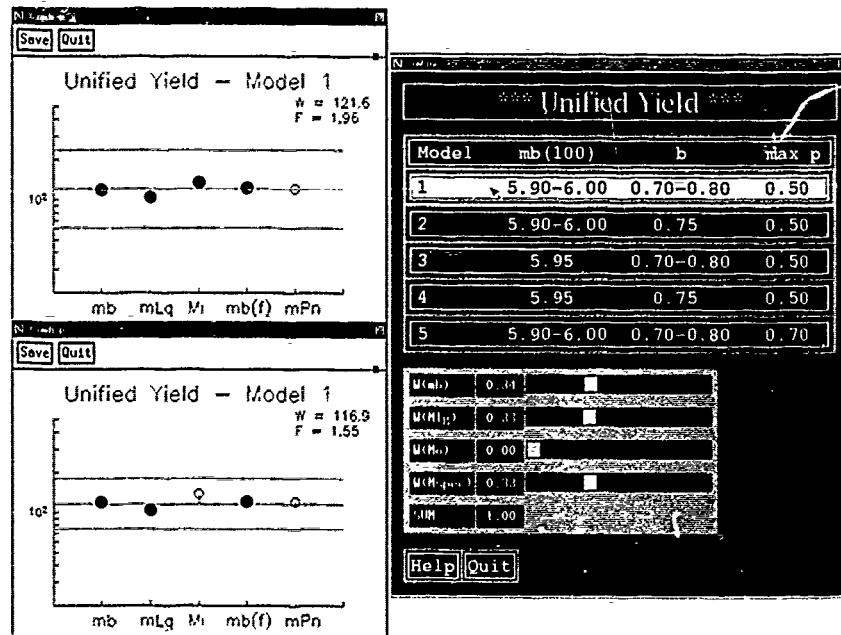


Figure 28.

Comparison of unified yield estimates (W) and associated uncertainties (F) obtained with (top) and without (bottom) the surface wave moment tensor magnitude.



Given an optimum seismic estimate of unified yield and the associated uncertainty, the analyst can next proceed to assess whether this

estimate is consistent with the 150 kt threshold of the Threshold Test Ban Treaty (TTBT) by selecting the *Statistical Summary* option from the

FUNCTION menu. This module provides access to a variety of statistical compliance assessment tests developed by Mission Research Corporation (Gray *et al.* 1990), as indicated by the menu displayed in Figure 29. In this example, the analyst has requested a summary of the results of three single event compliance tests, producing the graphical summary shown in Figure 30, where the red areas under the distribution curves provide a measure of the probability of a violation of the 150 kt threshold. The formal statistical results are summarized in the boxes in the upper left hand corners of these figures, and it can be seen that the results of each of these three tests indicate that the seismic data are consistent with a yield of less than 150 kt at a specified false alarm rate of less

Figure 29. Statistical assessment menu.

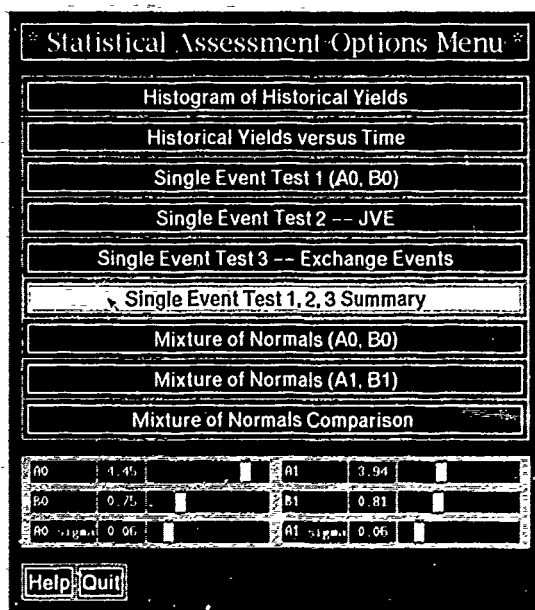
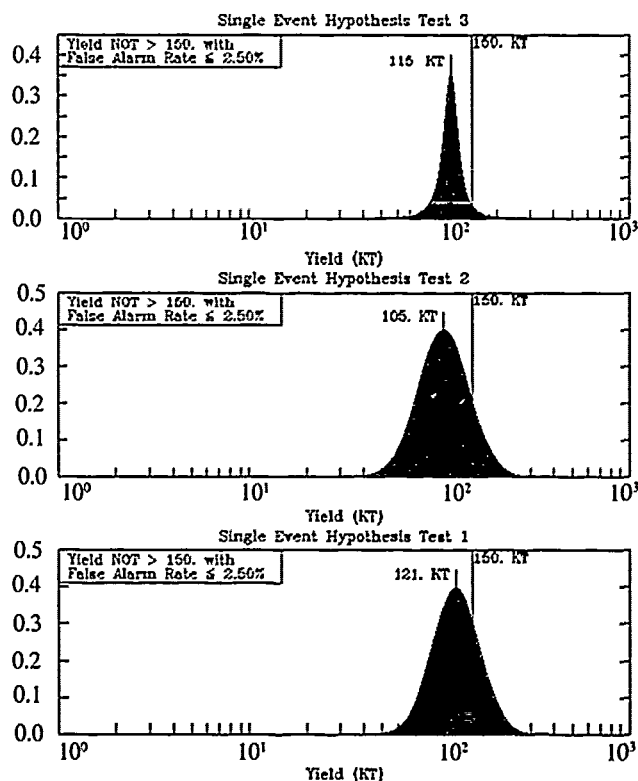


Figure 30.

Comparison of the results of three different tests of seismic compliance of the current event with the 150-kt threshold of the TTBT.



than 2.5 percent. The resolving power of such tests can be illustrated by considering the outcome which would have resulted if these same seismic data had been observed from a test below the water table at NTS. In this case, the Shagan m_b /yield relation would be replaced by (Murphy, 1981):

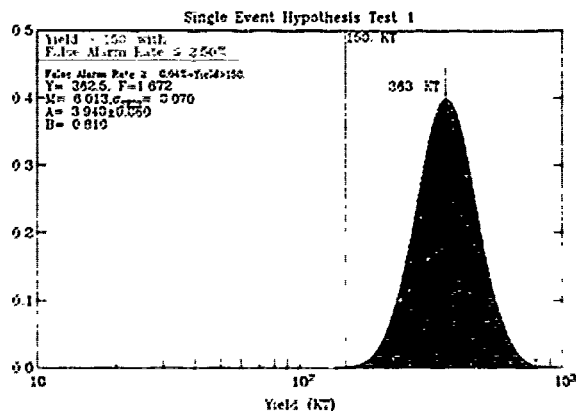
$$m_b = 3.94 + 0.81 \log W$$

resulting in the revised Test 1 outcome shown in Figure 31. It can be seen that under this hypothesis, the yield estimate would be 363 kt and it would be concluded that this explosion violated the 150 kt limit of the TTBT. Thus, this simple example graphically illustrates the importance of the test site magnitude bias effect which has received such intense study since the

initial negotiation of the TTBT.

Having completed the formal analysis, the *Spreadsheet* option from the FUNCTION menu

Figure 31. *Compliance test result (Test 1) for the scenario in which the current event data were observed from an explosion below the water table at NTS.*



can be used to provide a less formal environment for evaluating the seismic yield estimate for the current event in the context of the results obtained from analyses of previous explosions at that test site, as well as any available independent yield calibration data, as illustrated in Figure 32. In this display, the four individual seismic yield estimates and corresponding unified yields are listed for forty of the largest Shagan River explosions, together with selected calibration yields (W(Bocharov)), taken here for the purposes of illustration to be the three high yield values published by Bocharov *et al.* (1988). The ratios of the unified seismic to calibration yields are listed in

the last column, together with the average offset (Avg Bias) and uncertainty (F) inferred from these limited calibration data. For the nominal magnitude/yield relations listed at the top of this display, the average offset is a factor of 1.07 with an associated F factor of 1.25. Figure 33 shows the result of interactively adjusting each magnitude/yield relation in such a manner that the individual average offsets are minimized. It can be seen that these modifications eliminate the average bias in the unified seismic yield estimate (i.e., Avg Bias = 1.00) and reduces the F factor to 1.20. This example illustrates how the spreadsheet module provides a capability for the analyst to rapidly

Figure 32. Spreadsheet summary comparison of seismic yield estimates for the current event (09/14/88) with those obtained for selected previous Shagan River explosions.

| | H | I | H | I | Q | R | |
|-----------|--------|--------|--------|----------|---------|-------------|-------|
| Magnitude | Hb | Hlg | Ho | Hspec | | | |
| Slope | 0.75 | 0.75 | 1.00 | 0.75 | | | |
| Intercept | 4.45 | 4.45 | 5.00 | 4.45 | | | |
| Weight | 0.25 | 0.25 | 0.25 | 0.25 | | | |
| Event | W(Hb) | W(Hlg) | W(Ho) | W(Hspec) | W(Unif) | W(Bocharov) | Wu/We |
| 1/15/65 | 88.44 | | | 94.91 | 91.62 | | |
| 11/30/69 | 131.83 | 133.05 | | 118.03 | 127.45 | 125.00 | 1.02 |
| 11/02/72 | 190.55 | 167.0 | | 255.86 | 201.37 | 165.00 | 1.22 |
| 12/10/72 | 135.94 | 156.07 | | 125.12 | 138.46 | 140.00 | 0.99 |
| 7/23/73 | 215.44 | 212.16 | | 240.62 | 222.39 | | |
| 12/14/73 | 85.77 | 77.27 | | 69.40 | 77.19 | | |
| 6/11/78 | 85.77 | 54.12 | 128.82 | 75.39 | 81.94 | | |
| 8/29/78 | 100.00 | 119.86 | 81.28 | 100.93 | 99.58 | | |
| 9/15/78 | 88.44 | 87.90 | 112.20 | 93.47 | 95.02 | | |
| 11/29/78 | 120.23 | 106.01 | 120.23 | 106.01 | 112.89 | | |
| 6/23/79 | 184.78 | 138.46 | 177.83 | 184.78 | 170.28 | | |
| 7/07/79 | 91.20 | 105.68 | 75.86 | 97.27 | 91.83 | | |
| 8/04/79 | 140.17 | 158.98 | 186.21 | 183.09 | 166.02 | | |
| 8/18/79 | 153.70 | | 104.71 | 148.59 | 133.73 | | |
| 10/28/79 | 116.59 | 137.62 | 194.98 | 114.11 | 137.46 | | |
| 12/02/79 | 100.00 | 90.09 | 138.04 | 106.01 | 107.15 | | |
| 12/23/79 | 168.53 | | 79.43 | 163.93 | 129.95 | | |
| 9/14/80 | 251.19 | | 213.80 | 213.47 | 225.48 | | |
| 9/13/81 | 127.84 | 165.45 | 181.97 | | 156.72 | | |
| 10/18/81 | 106.33 | 111.00 | 144.54 | | 119.49 | | |
| 12/27/81 | 173.78 | 144.99 | 154.88 | | 157.44 | | |
| 4/25/82 | 113.07 | 148.14 | 144.54 | | 134.28 | | |
| 12/05/82 | 153.70 | 112.37 | 154.88 | | 138.82 | | |
| 6/12/83 | 113.07 | 145.88 | 199.53 | | 148.75 | | |
| 10/06/83 | 94.04 | 77.51 | 186.21 | | 110.72 | | |
| 10/26/83 | 144.54 | 116.23 | 213.80 | | 153.15 | | |
| 7/14/84 | 131.83 | 138.04 | 190.55 | | 151.36 | | |
| 10/27/84 | 202.61 | 149.97 | 173.78 | | 174.14 | | |
| 12/16/84 | 158.49 | 134.28 | 229.09 | | 169.56 | | |
| 12/28/84 | 94.04 | 110.32 | 79.43 | | 93.76 | | |
| 9/14/88 | 131.83 | 106.01 | 123.88 | 119.12 | 119.83 | | |
| | | | | | | Avg Bias | 1.07 |
| | | | | | | F | 1.25 |

Figure 33. Spreadsheet summary illustrating the results of interactively modifying the designed magnitude/yield relations.

| Magnitude | Mb | Mlg | Mo | Mspec | | | |
|-----------|--------|--------|--------|----------|---------|-------------|-------|
| Slope | 0.75 | 0.75 | 1.00 | 0.75 | | | |
| Intercept | 4.47 | 4.47 | 5.00 | 4.48 | | | |
| Weight | 0.25 | 0.25 | 0.25 | 0.25 | | | |
| Event | M(Mb) | M(Mlg) | M(Mo) | M(Mspec) | M(Unif) | M(Bocharov) | Wa/Wc |
| 1/15/65 | 83.18 | | | 85.56 | 84.85 | | |
| 11/30/69 | 123.97 | 125.12 | | 107.65 | 118.64 | 125.00 | 0.95 |
| 11/02/72 | 179.20 | 157.52 | | 233.35 | 187.45 | 165.00 | 1.14 |
| 12/10/72 | 127.84 | 146.78 | | 114.11 | 128.89 | 140.00 | 0.92 |
| 7/23/73 | 202.61 | 199.53 | | 219.45 | 207.01 | | |
| 12/14/73 | 80.66 | 72.67 | | 63.29 | 71.85 | | |
| 6/11/78 | 80.66 | 50.89 | 128.82 | 68.76 | 77.65 | | |
| 8/29/78 | 94.04 | 112.72 | 81.28 | 92.04 | 94.37 | | |
| 9/15/78 | 83.18 | 82.67 | 112.20 | 85.24 | 90.05 | | |
| 11/29/78 | 113.07 | 99.69 | 120.23 | 96.68 | 106.99 | | |
| 6/23/79 | 173.76 | 130.22 | 177.83 | 168.53 | 161.37 | | |
| 7/07/79 | 85.77 | 99.39 | 75.86 | 88.72 | 87.03 | | |
| 8/04/79 | 131.83 | 149.51 | 186.21 | 166.88 | 157.34 | | |
| 8/18/79 | 144.54 | | 104.71 | 135.52 | 127.06 | | |
| 10/28/79 | 109.65 | 129.42 | 194.98 | 104.07 | 130.27 | | |
| 12/02/79 | 94.04 | 84.72 | 138.04 | 96.68 | 101.55 | | |
| 12/23/79 | 158.49 | | 79.43 | 149.51 | 123.47 | | |
| 9/14/80 | 236.23 | | 213.80 | 194.69 | 214.23 | | |
| 9/13/81 | 120.23 | 155.60 | 181.97 | | 150.43 | | |
| 10/18/81 | 100.00 | 104.39 | 144.54 | | 114.70 | | |
| 12/27/81 | 163.43 | 135.35 | 154.88 | | 151.12 | | |
| 4/25/82 | 106.33 | 139.32 | 144.54 | | 128.89 | | |
| 12/05/82 | 144.54 | 105.68 | 154.88 | | 133.25 | | |
| 6/12/83 | 106.33 | 137.19 | 199.53 | | 142.78 | | |
| 10/06/83 | 88.44 | 72.89 | 186.21 | | 106.28 | | |
| 10/26/83 | 135.94 | 109.31 | 213.80 | | 147.01 | | |
| 7/14/84 | 123.97 | 129.82 | 190.55 | | 145.29 | | |
| 10/27/84 | 190.55 | 141.04 | 173.78 | | 167.15 | | |
| 12/16/84 | 149.05 | 126.28 | 229.09 | | 162.76 | | |
| 12/28/84 | 88.44 | 103.75 | 79.43 | | 90.00 | | |
| 9/14/83 | 123.97 | 99.69 | 123.68 | 108.64 | 113.57 | | |
| Avg Bias | | | | | | | 1.00 |
| F = | | | | | | | 1.20 |

explore the effects of alternate hypotheses on the seismic yield estimation process.

The sample analysis session described above has provided an overview of some of the capabilities which are currently available within the Yield Estimation System. As was evident from the menu structures shown in the graphical dis-

plays, there are, in addition, many other features which were not exercised here in order to hold the description to a manageable length. However, the complete system is currently operational at the DARPA CSS where it can be exercised over its entire range of functionality.

4 Summary and Future Plans

4.1 Summary

In this report we have presented a brief summary of the current status of the ongoing research investigations directed toward the development of a comprehensive new seismic yield estimation system for underground nuclear explosions. More specifically, a preliminary prototype version of this system, which is currently operational at the DARPA CSS, has been described in detail and its functionality has been graphically illustrated through a sample application to the seismic data recorded from a selected explosion.

The software system design criteria were reviewed in Section 2, where the characteristics of the data, analysis tools, database relations and graphical user interface were described in the context of their integration into a comprehensive system for seismic yield estimation and compliance assessment. This discussion included an overview of the conceptual model for the system and provided a description of how the prototype version has been implemented in a Sun color workstation environment using software built upon the framework of the X Window graphics and Oracle database management systems.

This was followed in Section 3 by a demonstration of system capabilities in which a complete processing session was graphically illustrated using data recorded from the Soviet JVE explosion of 14 September 1988. In this presenta-

tion, reproductions of the actual workstation screens encountered by an analyst in such a session were used as a framework for describing the simple menu structure on which the graphical user interface has been developed. Among other features, this demonstration illustrated the manner in which available test site information is presented to the analyst in the context of a SPOT satellite image of the test site, in a format which permits the analyst to interact digitally with the image in a workstation environment to create overlays to and cross-sections through the image to display event locations, topography, surface and subsurface geologic data and a variety of geophysical parameters of potential interest in yield estimation analysis. In addition, this sample session was used to illustrate the capabilities provided by the system which permit the analyst to interact with the recorded seismic data to process it and extract the various magnitude measures of interest, to formally combine these seismic measures of source size to obtain an optimum measure of explosion yield and quantitative measures of the associated uncertainty and to statistically assess the consistency of this seismic yield estimate with any existing treaty thresholds or other yield levels of particular interest.

4.2 Future Plans

Now that a preliminary working prototype has been successfully implemented, the research

effort is beginning to focus on the extension of the system to encompass data from a wider range of explosion test sites and stations and on the development of a semi-automated documentation module. More specifically, the following system modifications are planned for the next phase of system development:

- The system will be extended to incorporate explosions at the Soviet Novaya Zemlya test site. This addition will include a comprehensive seismic database consisting of all available digital seismic data recorded from these explosions at stations of the USAEDS, GDSN, NORSAR, CDSN and IRIS networks, as well as a test site information interface based on a SPOT satellite image of Novaya Zemlya.
- A new module will be added to the YES which will be designed to permit the analyst to

validate and process the regional seismic data recorded at the Designated Seismic Stations (DSS) provided for in the 1990 Protocol to the TTBT.

- The statistical yield estimation and assessment modules in the current version of the YES will be modified to incorporate any supplemental information resulting from CORRTX yield estimation activity or on-site inspections of the type provided for in the 1990 Protocol to the TTBT.
- A semi-automatic event report generation module will be added to the YES which will provide comprehensive graphical and text documentation of the yield estimation analyses conducted for any selected explosion.

Acknowledgements

The authors would like to take this opportunity to acknowledge the contributions to this project by T.J. Bennett and A.K. Campanella of S-CUBED, W.L. Rodi of Massachusetts Institute of Technology, W. Leith of the U.S. Geological Survey, G.D. McCartor of Mission Research Corpora-

tion and H.L. Gray of Southern Methodist University. Juanita Jenab of S-CUBED deserves special mention for her expert assistance in the integration of the text and graphics required for the preparation of this report.

References

- Anderson, J., W. E. Farrell, K. Garcia, J. Given, and H. Swanger (1990). Center for Seismic Studies Version 3 Database: Schema Reference Manual. Center for Seismic Studies Technical Report C90-01, September, 1990.
- Bocharov, V. S., S. A. Zelentsov and V. N. Mikhailov (1989), "Characteristics of 96 Underground Nuclear Explosions at the Semipalatinsk Test Site," *Atomic Energy (Atomnaya Energiya)*, 67, 3.
- Gray, H.L., W.A. Woodward and G.D. McCartor (1990), "Statistical Issues Concerning Testing for Compliance to the TTBT", paper presented at 12th Annual DARPA/GL Seismic Research Symposium, Key West, Florida.
- Herrin, E., E. P. Arnold, B. A. Bolt, G. E. Clawson, E. R. Engdahl, H. W. Freedman, D. W. Gordon, A. L. Hales, J. L. Lobdell, O. Nuttli, C. Romney, J. Taggart, and W. Tucker (1968), "1968 Seismological Tables for P Phases," *Bull. Seism. Soc. Am.*, 58, pp. 1193-1241.
- Leith, W. (1989), "Three-Dimensional Geologic Modeling of the Shagan River Nuclear Test Site," paper presented at the DARPA/AFTAC Annual Seismic Research Review, Patrick Air Force Base, Florida.
- Murphy, J. R. (1981), "P-Wave Coupling of Underground Explosions in Various Geologic Media," in *Identification of Seismic Sources - Earthquake or Underground Explosion, Proceedings of the NATO Advanced Study Institute*, D. Reidel Publishing Company.
- Murphy, J. R. (1989), "Network-Averaged Teleseismic P-Wave Spectra For Underground Explosions, II: Source Characteristics of Pahute Mesa Explosions," *Bull. Seism. Soc. Am.*, 79, pp. 16-31.
- Murphy, J.R. (1990), "A New System for Seismic Yield Estimation of Underground Explosions", paper presented at the 12th Annual DARPA/GL Seismic Research Symposium, Key West, Florida.
- Ringdal, F. (1983), "Magnitudes from P Coda and L_g Using NORSAR data," in NORSAR Semi-annual Technical Summary, 1 Oct 82 - 31 Mar 83, NORSAR Sci. Rep. No. 2-82/83, INTNF/NORSAR, Kjeller, Norway.
- Rodi, W. L. (1989), "A Mathematical Program For Unified Yield Estimation," S-CUBED Memorandum to DARPA Yield Technical Review Panel, December 22.
- Rodi, W. L. and J. R. Murphy (1990), "Numerical Experiments With Unified Yield Estimation," S-CUBED Technical Memorandum to DARPA Yield Technical Review Panel, April 19.